

Single molecule statistics and the polynucleotide unzipping transition

David K. Lubensky* and David R. Nelson†

Department of Physics, Harvard University, Cambridge, Massachusetts 02138

(Received 22 August 2001; published 6 March 2002)

We present an extensive theoretical investigation of the mechanical unzipping of double-stranded DNA under the influence of an applied force. In the limit of long polymers, there is a thermodynamic *unzipping* transition at a critical force value of order 10 pN, with different critical behavior for homopolymers and for random heteropolymers. We extend results on the disorder-averaged behavior of DNA's with random sequences [D. K. Lubensky and D. R. Nelson, Phys. Rev. Lett. **85**, 1572 (2000)] to the more experimentally accessible problem of unzipping a single DNA molecule. As the applied force approaches the critical value, the double-stranded DNA unravels in a series of discrete, sequence-dependent steps that allow it to reach successively deeper energy minima. Plots of extension versus force thus take the striking form of a series of plateaus separated by sharp jumps. Similar qualitative features should reappear in micromanipulation experiments on proteins and on folded RNA molecules. Despite their unusual form, the extension versus force curves for single molecules still reveal remnants of the disorder-averaged critical behavior. Above the transition, the dynamics of the unzipping fork is related to that of a particle diffusing in a random force field; anomalous, disorder-dominated behavior is expected until the applied force exceeds the critical value for unzipping by roughly 5 pN.

DOI: 10.1103/PhysRevE.65.031917

PACS number(s): 82.37.Rs, 87.14.Gg, 87.15.Aa

I. INTRODUCTION

Over the past decade, the experimental repertoire of biophysicists and structural biologists has expanded to include some remarkable micromanipulation techniques. These single molecule methods are a natural complement to more traditional scattering and spectroscopic measurements: Although they cannot ascertain structures at atomic resolution, they do give important information about the organization of disordered or strongly fluctuating systems, and they yield valuable estimates of the forces and energies that stabilize a given structure. Moreover, micromanipulation experiments on single molecules open a window into a rich and largely unexplored set of physical phenomena. One can now measure entire distributions of molecular properties, without the requirement for averaging over a macroscopic sample. Not only does the wealth of resulting data allow more stringent tests of ideas originally developed for macroscopic systems, it also has the potential to reveal entirely new behavior that was not discernible in aggregate results on heterogeneous populations of molecules [1–3]. In this paper, we study an example of a system—the *unzipping* of double-stranded DNA (dsDNA)—that shows exactly such novel response on the single molecule level. Our results are also directly applicable to the unzipping of a single RNA hairpin, and similar ideas can be applied to the force-induced denaturation of RNA's with more complicated secondary structures [3] and even to the stretching of folded proteins [4].

In the DNA unzipping problem, the two single strands of a double-stranded DNA molecule with a randomly chosen base sequence are pulled apart under the influence of a con-

stant force (Fig. 1). In addition to providing a surprisingly good description of protein-coding DNA [6], the assumption of a random sequence gives us an analytically tractable model; its solution then allows us to gain insight into a much broader class of systems. DNA unzipping thus serves as a model problem to illuminate the effect of sequence variation on a micromechanical experiment.

In a previous brief communication [5], we showed that the *average* extension versus force curve of an ensemble of random heteropolymers is markedly different from the corresponding curve for a homopolymer. Here, we move beyond averages over many different random sequences to examine the unzipping of a *single* dsDNA molecule. Interesting qualitative lessons emerge. Whereas a homopolymer gains considerable entropy by opening in response to a constant force, a heteropolymer unzips primarily for energetic reasons. In fact, the unzipping process is dominated by the presence of deep energy minima and is only mildly perturbed by thermal fluctuations. At any given applied force, the system will sit in the deepest available minimum; because the location of the minimum varies discontinuously with the applied force, the number of bases opened will show sharp jumps at certain force values. Moreover, the energy landscape is determined by the polymer's sequence, so the force-extension curve will be strongly sequence dependent.

A number of theorists have recently addressed aspects of dsDNA unzipping [7–15]; the mechanical properties of a single-stranded polynucleotide that can pair with itself have also received considerable attention [16–19]. With a few exceptions [13,19], however, this work has been restricted to the study of homopolymers, and thus does not overlap directly with the results presented here.

Although our model is chosen more for its simplicity than for a clear correspondence to a particular experiment in the literature, several related experiments have nonetheless been

*Present Address: Bell Labs, Lucent Technologies, 700 Mountain Ave., Murray Hill, NJ 07974. Email address: lubensky@lucent.com

†Email address: nelson@cmt.harvard.edu

performed. Early studies by Lee and co-workers [20] were followed by the ground breaking work of Essevaz-Roulet, Bockelmann, and Heslot [21], who demonstrated the feasibility of mechanically denaturing single dsDNA molecules, and showed that many features of their results could be understood using equilibrium statistical mechanics. Subsequently, similar experiments have been performed using an atomic force microscope [22,23]. In contrast to our calculations, this work was done in an ensemble in which the positions of the two single-stranded ends are held fixed while an average force is measured. Because of subtleties associated with the statistical mechanics of single molecule systems, this *constant extension* ensemble is not equivalent in the usual sense to our *constant force* ensemble; the connection between the two will be discussed in more detail in Sec. VI. More recently, Liphardt and co-workers have mechanically unfolded several different short RNA molecules related to a domain of the *Tetrahymena thermophila* ribozyme [3]. Here, a bead tethered to a force-measuring optical trap was used both to impose an extension and, with feedback, to monitor extension at fixed force—precisely the situation of interest in this paper. Alternatively, a constant force could be directly applied using a magnetic bead in a constant magnetic field gradient [24].

In the remainder of this paper, we first, in Sec. II, describe in more detail the phase diagram of polynucleotide duplexes and show how a coarse-grained model of the unzipping transition can be derived from more microscopic descriptions of dsDNA. This model, which will form the basis of all subsequent calculations, is summarized in Eqs. (13) through (15). For the purposes of comparison, we derive in Sec. III some results on the unzipping of homopolymeric dsDNA. Section IV revisits in more detail the disorder-averaged force-extension curve examined in Ref. [5]. The bulk of our new results on single-molecule unzipping appear in Sec. V. We show that the equilibrium extension versus force curve of a single dsDNA molecule consists of a series of long plateaus followed by large jumps, and we derive a statistical description of this striking behavior. We also demonstrate that, despite its choppy appearance, such a curve contains hidden signatures of the smooth disorder-averaged behavior. Subsequent sections consider the relationship between the conjugate constant force and constant extension ensembles (Sec. VI) and give a brief overview of the dynamics of unzipping (Sec. VII). We point out that polynucleotide unzipping provides an experimental realization of the famous Sinai problem of thermally activated diffusion in a quenched random force field [25,26]. Anomalous, quasilocalized dynamics persist up to roughly 5pN above the unzipping transition. Finally, in Sec. VIII, we discuss the implications of DNA unzipping for micromanipulation experiments on more complicated systems. The Appendix gives a brief description of the numerical methods used to generate results discussed in the body of the paper.

II. THE MODEL

Figure 1 depicts the situation studied in this paper: One of the single strands from a double-stranded DNA molecule is

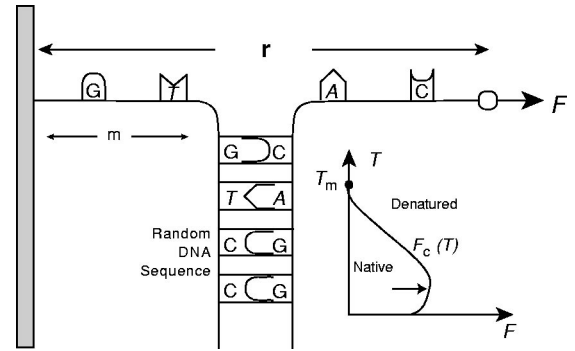


FIG. 1. Sketch of the DNA unzipping experiment. One of the single strands of a dsDNA molecule with a random base sequence is attached by its end to a solid surface, and the other is pulled away from the surface with a constant force \mathbf{F} . As a result, the double strand partially denatures, separating m base pairs ($m=2$ in the figure). The distance between the ends of the two single strands, or *extension*, is r . *Inset*: Schematic phase diagram in the temperature–pulling force (T – F) plane of a dsDNA molecule in three dimensions. At low enough T and F , the polymer is in the native, double-stranded phase. At the phase transition line $F_c(T)$, the DNA denatures and the two strands separate. Thermally induced *melting* occurs at zero force at a temperature T_m . As indicated by the arrow, this paper considers instead the *unzipping* transition, in which the phase transition line is crossed at nonzero F . The reentrance at low temperatures is predicted in Ref. [11].

attached to a glass slide, and the other to a bead on which a constant force \mathbf{F} is exerted. \mathbf{F} could be created, for example, with magnetic tweezers, which have been used to exert constant piconewton-scale forces over hundreds of microns [24]. Optical tweezers or atomic force microscopes (AFM) with appropriate feedback can create a similar effect [3,27]. As a result of the applied force, the DNA partially “unzips,” breaking m bonds. As long as the force-elongation curve of the liberated single-stranded DNA is known, m can be related to the distance r between the ends of the two single strands, which is easily measured. Our main goal is to understand how the *equilibrium* ensemble average $\langle m \rangle$ (where the angle brackets indicate an average over thermal noise) depends on F and on the base sequence of the DNA strand.

In certain limiting cases, the dependence of m on F is easy to understand. One might expect that at large enough forces the dsDNA will unzip completely, whereas for very small forces at most a few bases will open. We show below that these two regimes are separated by a sharp first-order phase transition. Below the critical force F_c , only a finite number of bases at the end of the double strand are pulled open; in the thermodynamic limit of an infinitely long DNA molecule, the pulling force thus has no effect on the *fraction* of open bases, which remains very small in physiological conditions. Above F_c , the entire molecule unzips, and the fraction of open bases jumps discontinuously to one. This phase diagram is sketched in the inset to Fig. 1. As F approaches F_c from below, the number m of unzipped bases at the end of the molecule diverges. Because this divergence is entirely a surface phenomenon, the unzipping transition can be thought of as the one-dimensional analog of a continuous wetting transition [28].

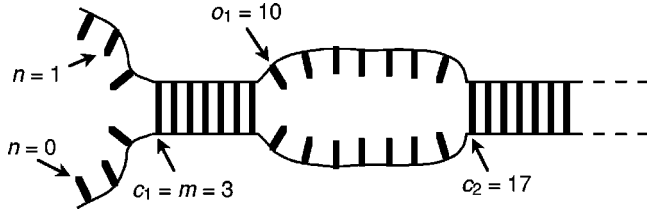


FIG. 2. Definition of the variables c_i and o_i in the Ising-like model [Eq. (1)]. In this figure, three bases are open at the end of the dsDNA. Counting the first open base as $n=0$, the location of the first closed base is then $c_1=3$. Similarly, the next open base is at $o_1=10$.

The effect of base sequence on the force-elongation curve is less straightforward. We can gain some insight into the role of a variable sequence by considering the problem of unzipping a DNA molecule where each successive base is chosen at random, with at most short-ranged correlations between bases. Although the sequence of protein-coding DNA is certainly not random in any strict sense, it nonetheless appears to many statistical criteria to fit this description (up to a length scale set by the sequence's mosaic structure) [6]. Deviations from randomness that escape these tests presumably involve fairly subtle multipoint correlations. Although the structure of the protein for which the DNA codes is likely to depend on such correlations, the mechanical denaturation of the DNA itself, which depends only on the cumulative energy cost of opening m bases, should be relatively insensitive to them. Simulations of the more complicated problem of pulling on folded RNA's have shown good agreement with the predictions of a random model [19]. It is thus reasonable, at least as a first approximation, to take the DNA sequence being unzipped to be random and uncorrelated. In the remainder of this section, we develop a mathematical description of the unzipping of such a DNA sequence by a constant force.

A. Semimicroscopic models

The bulk thermally driven *melting* transition of dsDNA (see Fig. 1) can be described at varying levels of detail by a number of models, all of which are expected to give the same universal behavior on long enough length scales. One popular choice is an Ising-like description, in which a base pair is taken to be in one of two discrete states—open or closed. By convention, the free energy of an unconstrained base pair in the open state is set to zero. A melted stretch of single-stranded DNA flanked by two unmelted regions must form a closed loop, and a loop factor accounts for the loss of entropy caused by this constraint [29]. The Hamiltonian of a semi-infinite strand can be written as a sum of (free) energies associated with successive paired and unpaired regions:

$$\mathcal{H}_1 = \sum_i \left\{ \left[\sum_{n=c_i}^{o_i-1} \varepsilon_n \right] + 2J + f(c_{i+1} - o_i) \right\}. \quad (1)$$

Here base positions are indexed by $n \in \{0, 1, 2, \dots\}$, and the i th closed and open sections start at base numbers c_i and o_i , respectively (see Fig. 2). Each base pair gains an energy ε_i

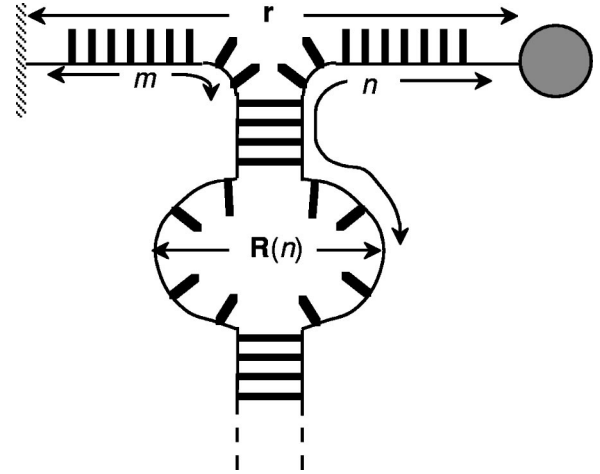


FIG. 3. Definition of the variables in the continuum model [Eq. (2)]. The distance between the ends of the two single strands (the *extension*) is r , and the number of open bases is m . The bases are indexed by n ; the separation between the two single strands at the n th base pair from the end is given by $\mathbf{R}(n)$.

from being closed; sequence-dependent stacking interactions can be included by adding an additional energy $\varepsilon_{n,n+1}$ [30]. For the case of a random DNA sequence, the ε_i are independent random variables. The energy $2J$ per open section gives the energetic cost of initiating a melted region, and $f(c_{i+1} - o_i) \propto \ln 2(c_{i+1} - o_i)$ is the entropic penalty associated with forming a closed loop of length $2(c_{i+1} - o_i)$. If there are open bases at the end of the molecule, before the first closed section, they are counted as the zeroth open section and do not incur any loop penalty. The model's partition function is a sum over all possible opening and closing points, $Z_1 = \sum_{0 \leq c_1 < o_1 < \dots < c_n < o_n \dots} \exp(-\mathcal{H}_1/k_B T)$.

Alternatively, some models of the melting transition are written in terms of the position of each base in three-dimensional space [31]. In the continuum limit, the simplest such description of a dsDNA of finite length N has the Hamiltonian

$$\mathcal{H}_C = \int_0^N dn \left\{ \frac{k_B T d}{4ab} \left(\frac{d\mathbf{R}}{dn} \right)^2 + V_n[\mathbf{R}(n)] \right\}, \quad (2)$$

where $\mathbf{R}(n)$ is the relative displacement of the two single strands at base pair n , d is the spatial dimension, a is the backbone length of a chemical monomer along a single strand, and b is the Kuhn length of single-stranded DNA (see Fig. 3); the factor of $1/ab$ appears instead of the more usual $1/b^2$ [32] because n indexes base pairs rather than Kuhn segments. We will usually be interested in the limit $N \rightarrow \infty$ of a semi-infinite polymer, just as for the Ising-like model. By convention, $\mathbf{R}(n) = \mathbf{0}$ when the n th set of bases are paired. Because we will be especially interested in the distance between the ends of the two single strands, it is useful to define the *extension*

$$\mathbf{r} \equiv \mathbf{R}(0). \quad (3)$$

The first term in Eq. (2) describes the entropic elasticity of the single strands [32] and thus has the same effect as the loop factors in the Ising-like model. The second term accounts for the attractive interactions between the two single strands. Coarse-grained over a number of bases, they are described by a phenomenological potential energy term

$$V_n[\mathbf{R}(n)] = [1 + \tilde{\eta}(n)]h[\mathbf{R}(n)]. \quad (4)$$

Here h is a short-ranged attractive potential, and the variation with base sequence of the strength of the attraction between strands is described by $\tilde{\eta}(n)$. Standard methods show that the continuum partition function $Z_C(\mathbf{R}, N) \equiv \int \mathcal{D}[\mathbf{R}'(n)] \exp(-\mathcal{H}_C[\mathbf{R}']/k_B T)$ obeys an imaginary time Schrödinger equation [32].

Either model can readily be extended to include a force pulling apart the double-stranded molecule. We first show explicitly how this can be done neglecting long-ranged interactions (e.g., excluded volume or base-pairing interactions) within the liberated single strands. Subsequently, we will argue that including such effects will lead to only minor changes in our results near enough to the transition. A constant force acting at the end of the DNA ($n=0$) to separate the two single strands contributes an energy that is linear in their separation. In the case of the continuum model (2), one must thus add a term to the Hamiltonian of the form

$$\mathcal{H}_{C,\text{pull}}(\mathbf{F}) = -\mathbf{F} \cdot \mathbf{r} = \int_0^N dn \mathbf{F} \cdot d\mathbf{R}/dn. \quad (5)$$

In writing the second equality, we have neglected the effect of the other end of the dsDNA at $N=\infty$; with a physical polymer of finite length N , this approximation should be valid as long as the number of open bases $m \lesssim N$, so that $\mathbf{R}(N) \approx \mathbf{0}$.

Unlike the continuum model, the Ising-like model does not keep track of the positions of the open bases. We must thus take an alternative view of the effect of an unzipping force. The last equality of Eq. (5) gives a hint of how to do this. Suppose that, as in Fig. 2, the first closed section of dsDNA starts at base c_1 , so that $m=c_1$ bases are unzipped by the force. In the discrete Ising-like model, each liberated single strand can be described as a string of m individual monomers. The n th such monomer contributes a displacement \mathbf{u}_n^a or \mathbf{u}_n^b to the total end-to-end distance of the single strand, where the superscripts distinguish the two strands. The energy of unzipping is thus $-\mathbf{F} \cdot \mathbf{r} = -\sum_{n=0}^m \mathbf{F} \cdot \mathbf{u}_n^a + \sum_{n=0}^m \mathbf{F} \cdot \mathbf{u}_n^b$. Note that there is no reason to extend the sums over n to infinity; the positions of base pairs beyond the first closed pair have no effect on the end-to-end distance $\mathbf{r} \equiv \mathbf{R}(0)$. We would now like to trace over the \mathbf{u} 's to obtain a contribution to the Hamiltonian that depends only on the number of open monomers $m=c_1$. The precise result will depend on the model used to describe the elastic properties of a single-stranded monomer. For any reasonable choice, however, the traces over the different \mathbf{u} 's must decouple, leading to a free energy of the form $2mg(F)$. Here $g(F)$ is the change in free energy of a single-stranded monomer caused by applying a tension F ; by definition, $g(0)=0$. Be-

cause the monomers gain energy by aligning with the pulling force, $g(F)$ decreases with increasing F . For example, the continuum model Hamiltonian (2) is quadratic in $d\mathbf{R}/dn$ and thus describes a polymer that responds linearly to an arbitrarily large force. Such a Gaussian model results in a $g(F)$ that is quadratic in F :

$$g(F) = -\frac{a}{b} \frac{F^2 b^2}{2dk_B T} \quad (\text{Gaussian}). \quad (6)$$

Similarly, for an inextensible freely jointed chain, one finds [33]

$$g(F) = -\frac{a}{b} k_B T \ln \left[\frac{k_B T \sinh(Fb/k_B T)}{Fb} \right] \quad (\text{Freely jointed}). \quad (7)$$

In these equations, a is again the backbone distance between bases; the factor of a/b is necessary because $g(F)$ is defined as the free energy per chemical monomer, not per Kuhn length. More generally, if the force $F_{ss}(x)$ exerted by the single-stranded polymer as a function of the extension x per base can be measured, then

$$g(F) = \int_0^{x(F)} F_{ss}(x') dx' - Fx(F) = -\int_0^F x(F') dF', \quad (8)$$

where $x(F)$ is the inverse function of $F_{ss}(x)$.

Regardless of the exact form of $g(F)$, the effect of an unzipping force can be included in the Ising-like model by adding a term to the Hamiltonian (1) that gives the free energy of the unzipped monomers under tension. Because $m=c_1$, we have $\mathcal{H} = \mathcal{H}_1 + \mathcal{H}_{1,\text{pull}}$ with

$$\mathcal{H}_{1,\text{pull}}(F) = 2c_1 g(F). \quad (9)$$

Since $g(F) < 0$, this term favors increasing c_1 , and thus unzipping the dsDNA.

B. Reduction to one degree of freedom

Semimicroscopic models such as those just discussed contain far more details than are necessary to describe the unzipping transition. Our calculations would simplify if we could integrate out nonessential degrees of freedom to obtain a description that focuses on the number of unzipped bases m . The full partition function of the Ising-like model is a sum over all of the closing and opening points c_1, c_2, c_3, \dots and o_1, o_2, o_3, \dots . Among these parameters, the only one that determines the number of bases that have been unzipped is c_1 . Hence we focus on a constrained partition function with $c_1=m$ fixed,

$$Z_1^0 \exp \left[-\frac{\mathcal{E}(m)}{k_B T} \right] \equiv \sum_{m=c_1 < o_1 < c_2 < o_2 < \dots < c_n < o_n < \dots} \times \exp \left[-\frac{\mathcal{H}_1 + \mathcal{H}_{1,\text{pull}}(F)}{k_B T} \right], \quad (10)$$

where the partition function

$$Z_I^0 = \sum_{0=c_1 < o_1 < \dots < c_n < o_n \dots} \exp[-\mathcal{H}_I/k_B T - \mathcal{H}_{I,\text{pull}}(F)/k_B T]$$

with c_1 constrained to be zero is included so that $\mathcal{E}(0)=0$. This expression defines the function $\mathcal{E}(m)$; it can be introduced in a similar manner in the continuum model, by adding the constraint $\mathbf{R}(m)=\mathbf{0}$ to the partition function $Z_C(\mathbf{R},N) \equiv \int \mathcal{D}[\mathbf{R}'(n)] \exp(-\mathcal{H}_C/k_B T - \mathcal{H}_{C,\text{pull}}/k_B T)$ and replacing the attractive potential V_n with a hard core repulsion for $n < m$. $\mathcal{E}(m)$ gives the change in free energy from unzipping exactly m bases under the influence of a force F . It can be written as the sum of the free energy $2mg(F)$ of the m liberated base pairs and of the change in free energy of the dsDNA when it is shortened by m base pairs. This second term takes account of any fluctuations that open base pairs beyond the first closed base c_1 and is independent of F . For homopolymeric DNA, this term takes the form $-mg_0$, where $g_0 < 0$ is the average free energy per base pair of dsDNA. Once sequence heterogeneity is present, however, we must include sequence-dependent deviations from the average. If the deviation from the average on opening the n th base is $\eta(n)$, then $\mathcal{E}(m)$ can be written as

$$\mathcal{E}(m) = [2g(F) - g_0]m + \sum_{n=1}^m \eta(n). \quad (11)$$

Consider now the statistics of the random contribution $\eta(n)$, assuming that the underlying DNA sequence is random and uncorrelated. The function $\eta(n)$ reflects this bare sequence [represented by $\tilde{\eta}$ in the continuum model potential (4)] dressed by thermal fluctuations. As long as the dsDNA is well below its melting temperature, one expects that η will be a random variable with correlations that decay on the scale of the finite correlation length of the dsDNA. If we are only interested in long-length-scale properties, we can thus take η to be Gaussian white noise. It is convenient to define a quantity

$$f \equiv 2g(F) - g_0; \quad (12)$$

f is positive below the unzipping transition and negative above it. Passing to the continuum limit, we can then write

$$\mathcal{E}(m) = fm + \int_0^m dn \eta(n), \quad (13)$$

where $\eta(n)$ is a zero-mean Gaussian random variable that satisfies

$$\overline{\eta(n)\eta(n')} = \Delta \delta(n-n'). \quad (14)$$

Here the overbar indicates a ‘‘disorder average’’ over different realizations of the random base sequence. The associated partition function is simply, up to an unimportant multiplicative constant,

$$Z = \int_0^\infty dm \exp\left(-\frac{\mathcal{E}(m)}{k_B T}\right). \quad (15)$$

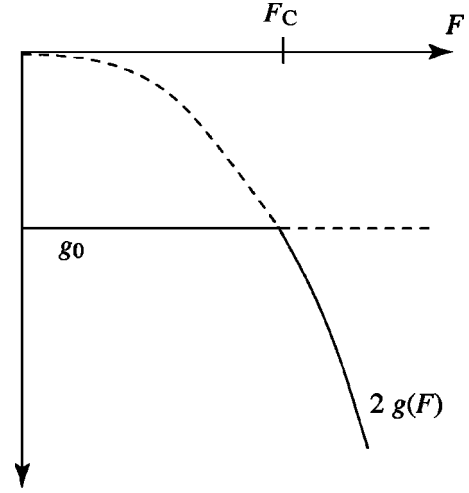


FIG. 4. Sketch of the bulk free energies per base pair g_0 of the zipped phase and $2g(F)$ of the unzipped phase as a function of the applied force F . These negative energies are measured relative to the free energy of a base pair at infinite separation with $F=0$. While g_0 is independent of F , $2g(F)$ decreases with increasing F . At a critical force value F_c , the zipped phase becomes unstable relative to the unzipped phase, and a phase transition occurs. The equilibrium free energy per base pair as a function of F is given by the solid curves; the discontinuous change in slope at F_c indicates a first-order transition.

Equations (13) through (15) define the basic model that we will study for the remainder of this paper. It is simple enough to allow a number of exact predictions, but still correctly captures the coarse-grained features of unzipping in the presence of sequence heterogeneity. It is not difficult to see that our model shows a sharp unzipping transition: At $F=0$, $f=2g(0)-g_0=-g_0$ is positive. As the pulling force F is increased from 0, $g(F)$ becomes negative, and f decreases but remains positive. $\mathcal{E}(m)$ thus grows linearly for large m , and at most a finite number of bases near the end of the dsDNA can be unzipped. These do not contribute appreciably to the average free energy per base pair of a very long molecule, which remains g_0 as at zero force. As F increases and $g(F)$ becomes increasingly negative, however, f changes sign at some critical force value F_c satisfying

$$2g(F_c) = g_0. \quad (16)$$

Upon expanding about F_c we see that to leading order, $f \sim F_c - F$. For $F > F_c$, the average slope f of $\mathcal{E}(m)$ is negative, and $\mathcal{E}(m)$ tends towards negative infinity for large m . It is thus advantageous to unzip the dsDNA completely. With all base pairs unzipped, the average free energy per pair becomes $2g(F)$. The discontinuous slope at F_c of the free energy per base pair as a function of F (see Fig. 4) indicates that the bulk transition is first order. Surface quantities such as $\langle m \rangle$ will nonetheless diverge as the transition is approached, just as in a critical wetting transition near a conventional first-order phase transition [28]. The precise surface behavior in this one-dimensional system will be the subject of subsequent sections.

For dsDNA in physiological conditions, one can ignore the rare fluctuational openings of base pairs in the bulk and use published base pairing energies to estimate the parameter values in our model. The pairing energies typically vary between roughly $1k_B T$ and $3k_B T$ per base [34]; one thus finds $g_0 \sim 2k_B T$ and $\Delta \sim 1(k_B T)^2$. A typical Kuhn length for single-stranded DNA (ssDNA) is $b \sim 15 \text{ \AA}$ [33,35]; inserting this value into the freely jointed chain expression for $g(F)$ [Eq. (7)] gives a pulling force F of order 10 pN at the unzipping transition. As we shall see, the sequence randomness dominates when $|f| \lesssim \Delta/k_B T \sim k_B T$; randomness is hence important whenever there is appreciable unzipping in heterogeneous polynucleotide sequences in physiological conditions.

The model of Eqs. (13) through (15) is considerably more general than the semimicroscopic models from which we derived it. For example, once $g(F)$ has been ascertained [e.g. by measuring the force-extension curve of ssDNA in appropriate conditions [3,33,35] and using Eq. (8)], it can be used without reference to any underlying description of the ssDNA. In fact, many predictions of our model are independent of its exact form. Similarly, most models of dsDNA (or of RNA hairpins) can be used to define parameters g_0 and Δ ; all of the relevant information about the duplex is contained in these two numbers. We also expect that our description applies even when nonlocal interactions along the ssDNA backbone are allowed. All that is required is that the free energy of the ssDNA be proportional to m , so that a function $g(F)$ can be defined. For example, a polymer in a good solvent under tension can be described as a string of blobs [36]. Once m is larger than the blob size, as must occur close enough to the unzipping transition, the free energy of the single strands will be proportional to m . In fact, in physiological conditions and at the forces of order 10 pN required to unzip dsDNA, the blob size will be at most a few monomers, meaning that excluded volume interactions can be neglected entirely in a first approximation. Likewise, a model of single stranded polynucleotides with uniformly attractive, nonrandom base pairing interactions (tending to produce hairpins) predicts a free energy proportional to the number of bases in the strand [16]. This model agrees well with experimental force-extension curves for ssDNA. The same calculations show that the fraction of bases in the liberated single strands involved in intrastrand pairing interactions will be small at the unzipping transition. Sequence variation will further suppress such pairing: Because not all bases can pair with each other, it will generally be necessary to make a large loop in order to bring together two stretches of bases that can pair to form a stem. This means that more work must be done against the pulling force for the same gain in base pairing energy. Although it might still be possible for a stem region of atypically high GC content to pair in this way, in a truly random sequence the probability of finding such a region decays exponentially with its length.

C. Related physical systems

Although the main focus of this paper will be the mechanical unzipping of polynucleotide duplexes, our formalism also applies to other experiments and physical systems.

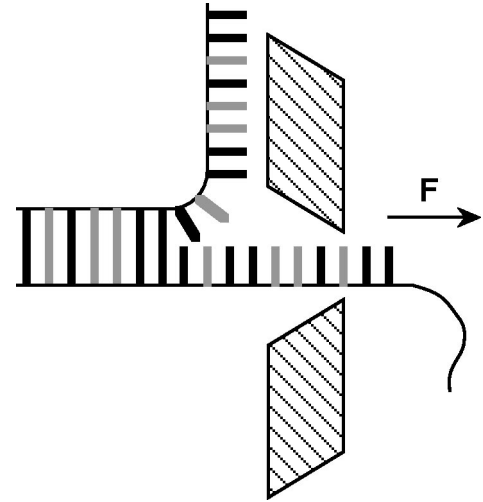


FIG. 5. Schematic of dsDNA unzipping through a narrow pore [37]. The pore is assumed to be large enough that single-stranded DNA, but not double-stranded DNA, can fit through it. Under the influence of an electric field or comparable force F , one single strand inserts into the channel and is gradually pulled through. As the strand is drawn through the pore, it must unzip from its complementary strand.

For example, an alternative method for unzipping DNA is to force one of the single strands through a very small pore by applying an electric field [37]. If the pore is so narrow that double-stranded DNA cannot fit through it, and if the applied field is strong enough, one of the single strands can enter the pore and be drawn through it, thereby unzipping the duplex (see Fig. 5). In this case, the analog of $g(F)$ is the electrostatic energy gained by the single strand passing through the pore, reduced by any entropic penalty the other single strand must pay due to confinement by parts of the pore or the adjoining walls [38]. Continuum models such as Eq. (2) are also commonly used to describe a number of other systems; in several of them, there is a natural analog to the pulling force F_c . Examples include the adsorption of a Gaussian random heteropolymer, where F_c maps directly to a force pulling the end of the polymer away from the adsorbing surface [39], and a flux line in a type II superconductor bound to a fragmented columnar defect [40], where F_c can be viewed as the magnetic field strength perpendicular to the defect. In addition, the Hamiltonian $\mathcal{H}_C + \mathcal{H}_{C,\text{pull}}$ bears a strong resemblance to models of the wetting transition in two dimensions in a wedge with angle close to 180° [41].

III. STATISTICAL MECHANICS OF HOMOPOLYMER UNZIPPING

Before tackling the more difficult problem of unzipping a double-stranded molecule with a random base sequence, we describe some results for a uniform sequence [5,9]. If the energy cost of opening each successive base pair is the same, then the deviation $\eta(n)$ from the average vanishes identically, and $\mathcal{E}(m) = fm$. Even if, as would be the case for an alternating base sequence, $\eta(n)$ is a nonzero periodic function, we expect that on scales longer than its period, $\eta(n)$ can safely be set to zero. In this section, we show explicitly

that the semimicroscopic continuum model discussed above [Eqs. (2) and (5)] gives results identical to those following from the simpler single degree of freedom description.

Equilibrium statistical mechanics in a linear potential is straightforward. The partition function of our minimal model is simply $Z = \int_0^\infty dm \exp(-mf/k_B T) = k_B T/f$, and the probability of opening exactly m bases is $(f/k_B T) \exp(-mf/k_B T)$. The equilibrium moments of m can be obtained from derivatives of the free energy $G(f) = -k_B T \ln Z$ with respect to f : $\langle m \rangle = \partial G / \partial f = k_B T/f$, $\langle m^2 \rangle - \langle m \rangle^2 = \partial^2 G / \partial f^2 = k_B T/f^2$, and so on. Recalling that $f \sim F_c - F$, we see that $\langle m \rangle$ exhibits a power law divergence near the unzipping transition;

$$\langle m \rangle \sim (F_c - F)^{-1} \quad (\text{homopolymer}). \quad (17)$$

The divergence of $\langle m \rangle$ has a simple origin: Although the absolute minimum of $\mathcal{E}(m)$ remains at $m=0$ everywhere below the transition, the system explores all configurations with $\mathcal{E}(m) \leq k_B T$, or equivalently $m \leq k_B T/f$; this of course suggests the same scaling for $\langle m \rangle$ found in the exact calculation. The homopolymer thus opens partially for $F < F_c$ entirely in order to gain *entropy*. We shall see in subsequent sections that a very different physical mechanism dominates in the unzipping of heteropolymers.

Connection to non-Hermitian delocalization

A different perspective on the mechanical denaturation of a homopolymer follows from viewing the energy $\mathcal{H}_C + \mathcal{H}_{C,\text{pull}}$ of the continuum model [Eqs. (2) and (5)] as an imaginary time quantum mechanical action. The partition function $Z(\mathbf{R}, N)$ of a strand of length N , subject to the constraint $\mathbf{R}(N) = \mathbf{R}$, satisfies the partial differential equation [32]

$$\frac{\partial Z}{\partial N} = \frac{b^2}{d} \left(\nabla_{\mathbf{R}} + \frac{\mathbf{F}}{k_B T} \right)^2 Z - \frac{V(\mathbf{R})}{k_B T} Z \equiv -\mathcal{L}(\mathbf{F})Z, \quad (18)$$

where the sequence-dependent function $V_N(\mathbf{R})$ is replaced by the N -independent potential $V(\mathbf{R})$ for a homopolymer. In order to avoid a proliferation of factors of a/b , we assume that the backbone distance a between chemical monomers is equal to the Kuhn length b . When $\mathbf{F} = \mathbf{0}$, Eq. (18) is just an imaginary-time Schrödinger equation. With the addition of a nonzero pulling force \mathbf{F} , the strict correspondence with conventional quantum mechanics is lost. Nonetheless, much can be learned by studying the evolution operator \mathcal{L} using the language of quantum mechanics. This avenue has been pursued for the formally identical problem of a flux line pinned to a defect in a type II superconductor [42]. In this section, we show explicitly that results from this more microscopic approach can be recovered from the simplified model embodied in Eqs. (13) through (15).

In analyzing Eq. (18), it is useful to view the force \mathbf{F} as a constant, imaginary vector potential. The ‘‘gauge transformation’’ operator

$$\mathcal{U}: \psi(\mathbf{R}) \mapsto \exp(\mathbf{F} \cdot \mathbf{R}/k_B T) \psi(\mathbf{R}) \quad (19)$$

can thus be used to relate the operator $\mathcal{L}(\mathbf{F})$ at a force \mathbf{F} to the Hermitian operator $\mathcal{L}(\mathbf{0})$:

$$\begin{aligned} \mathcal{L}(\mathbf{F}) &= \mathcal{U} \mathcal{L}(\mathbf{0}) \mathcal{U}^{-1}, \\ \mathcal{L}(\mathbf{0}) &= -\frac{b^2}{d} \nabla_{\mathbf{R}}^2 + \frac{V(\mathbf{R})}{k_B T}. \end{aligned} \quad (20)$$

Under the same transformation, the eigenfunctions $\psi_n^{\mathbf{F}}(\mathbf{R})$ of $\mathcal{L}(\mathbf{F})$ are given by

$$\psi_n^{\mathbf{F}}(\mathbf{R}) = \mathcal{U} \psi_n^{\mathbf{0}}(\mathbf{R}) = e^{\mathbf{F} \cdot \mathbf{r}/k_B T} \psi_n^{\mathbf{0}}(\mathbf{R}). \quad (21)$$

Equation (21) shows that exerting a nonzero force \mathbf{F} biases the eigenfunctions in the direction of the force. This transformation is valid as long as the new eigenfunction $\psi_n^{\mathbf{F}}$ satisfies the same boundary conditions as the untransformed eigenfunction. If we think of an isolated polymer in a box whose size tends towards infinity, the appropriate boundary conditions are that $\psi_n^{\mathbf{F}}$ be well behaved at infinity; given the form of \mathcal{U} , this is equivalent to demanding that the eigenfunction $\psi_n^{\mathbf{0}}(\mathbf{R})$ of the Hermitian problem decay at least as fast as $\exp(-FR/k_B T)$ for large $R = |\mathbf{R}|$. When this condition holds for the n^{th} eigenfunction, the corresponding eigenvalues of $\mathcal{L}(\mathbf{0})$ and $\mathcal{L}(\mathbf{F})$ will be identical, and the eigenfunctions will be related according to Eq. (21). Because, according to Eq. (18), the contribution of each eigenvalue λ_n to the partition function decays as $\exp(-\lambda_n N)$, the smallest eigenvalue λ_0 dominates in the limit of a very long polymer duplex. We are interested in conditions in which the dsDNA is stable in the absence of a pulling force; in this case, $\mathcal{L}(\mathbf{0})$, which describes the native, unpulled polymer, must have at least one bound state. The ground state eigenvalue $\lambda_0 < 0$ differs from the free energy per length g_0 of dsDNA introduced previously only by a factor of $k_B T$: $g_0 = k_B T \lambda_0$. Because $V(\mathbf{R})$ is a short-ranged potential, the ground state wave function $\psi_0^{\mathbf{0}}(\mathbf{R})$ should decay as $\exp(-\kappa_0 R)$ for large R , with the decay rate given by

$$\kappa_0 = \frac{1}{b} \sqrt{|\lambda_0| d} = \frac{1}{b} \sqrt{\frac{|g_0| d}{k_B T}}, \quad (22)$$

where d is the spatial dimension. When applied to the ground state wave function, the gauge transformation of Eq. (21) thus breaks down at a force of magnitude F_c given by

$$\frac{F_c}{k_B T} = \kappa_0 \Leftrightarrow F_c = \frac{k_B T}{b} \sqrt{\frac{|g_0| d}{k_B T}}. \quad (23)$$

It is natural to regard this force as the location of the unzipping transition. Indeed, one can show [42] that far from the ends of a long polymer, the probability that a given base pair will be separated by a displacement \mathbf{R} is $P_\infty(\mathbf{R}) = \psi_0^{\mathbf{F}}(\mathbf{R}) \psi_0^{-\mathbf{F}}(\mathbf{R})$. For $F < F_c$, the two gauge transformations cancel each other, and $P_\infty(\mathbf{R}) = [\psi_0^{\mathbf{0}}(\mathbf{R})]^2$. Thus, below F_c paired bases in the bulk of the dsDNA always stay near each other, and the polymer is below the unzipping transition (see Fig. 6). Conversely, above F_c , where the gauge transformation is no longer valid, the eigenfunctions $\psi_0^{\pm \mathbf{F}}$ are dominated

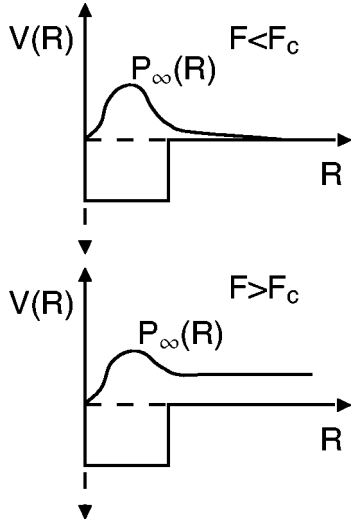


FIG. 6. Schematic of the base separation probability $P_\infty(R)$ below and above the first-order unzipping transition (the probability is expected to depend only on the radial distance R , not on angular coordinates). Below the transition, $P_\infty(R)$ decays quickly to zero beyond the range of the attractive potential $V(\mathbf{R})$. Above the transition, in contrast, it approaches a constant nonzero value as $R \rightarrow \infty$.

by \mathbf{F} and are extended. Indeed, one can demonstrate that they become plane waves as $R \rightarrow \infty$. The two single strands are then typically widely separated (Fig. 6), and the DNA is above an unzipping transition given by Eq. (23).

Upon inserting the expression for $g(F)$ [Eq. (6)] appropriate for the Gaussian single-stranded polymer into our previous criterion $2g(F_c) = g_0$, we obtain a value for the critical unzipping force F_c identical to Eq. (23). In fact, provided the duplex binding potential $V(\mathbf{R})$ vanishes as $R \rightarrow \infty$, $\psi_0^F(\mathbf{R})$ will approach a nonzero constant for large R above F_c . One can then read off $\lambda_0 = -b^2 F^2 / d(k_B T)^2$ directly from Eq. (18); the free energy above the transition is simply $k_B T \lambda_0 = 2g(F)$, a natural result given that above the unzipping transition the DNA is entirely in the single-stranded form. Within the present formalism, one can also obtain a closed-form expression for λ_0 , and hence for the free energy per monomer, below the unzipping transition. For $F < F_c$, the transformation (21) is valid, and $\lambda_0 = -b^2 \kappa_0^2(T) / d$, independent of F . Both the entropy, given by a derivative of $k_B T \lambda_0$ with respect to T , and the average extension per nucleotide in the bulk, given by a derivative of $k_B T \lambda_0$ with respect to F , change discontinuously at F_c (see Fig. 4). The bulk unzipping transition is thus first order, as is the case for the related problem of a single flux line torn away from a columnar defect in a type II superconductor [42].

Because $k_B T \lambda_0$ is the *bulk* free energy per monomer, its derivatives tell us nothing about the diverging surface precursors to the unzipping transition. To study surface effects within the quantum mechanical formalism, note that the probability that the ends of the two single strands are separated by a displacement $\mathbf{r} = \mathbf{R}(0)$ is given by [42]

$$P_0(\mathbf{r}) = \psi_0^F(\mathbf{r}) \simeq \exp\left[\frac{\mathbf{F} \cdot \mathbf{r}}{k_B T} - \kappa_0 |\mathbf{r}|\right], \quad (24)$$

where the last equality is valid outside the range of the potential $V(\mathbf{R})$. Focusing, for simplicity, on the case of one spatial dimension ($d=1$), and replacing the vectors \mathbf{R} and \mathbf{r} by the scalars R and r , it follows that the average distance $\langle r \rangle$ between the ends of the two single strands diverges as

$$\langle r \rangle = \frac{(\kappa_0 - F/k_B T)^{-2} + (\kappa_0 + F/k_B T)^{-2}}{(\kappa_0 - F/k_B T)^{-1} + (\kappa_0 + F/k_B T)^{-1}} \sim \frac{1}{F_c - F}. \quad (25)$$

Slightly more involved calculations [42] give the decay of the end-to-end distance as the bulk value is approached,

$$\langle R(n) \rangle = \langle r \rangle \exp\left(-\frac{n}{n^*}\right), \quad (26)$$

where $\langle R(n) \rangle$ is the average distance between the two single strands at base pair n . The healing length n^* diverges near F_c as

$$n^* = \frac{k_B T^2}{b^2(F_c^2 - F^2)} \sim \frac{1}{F_c - F}. \quad (27)$$

To check these results against the single degree of freedom model defined by Eqs. (13)–(15), one must translate the number of unzipped base pairs m into a distance r between the ends of the two single strands. When m base pairs have been unzipped, r is simply the end-to-end distance of a Gaussian polymer of length $2m$ subject to a force F ; it thus has distribution [36]

$$P_0(r|m) = \frac{1}{\sqrt{4\pi m b^2}} \exp\left\{-\frac{[r - 2mb^2 F/k_B T]^2}{4mb^2}\right\}. \quad (28)$$

The probability that precisely m base pairs have been unzipped is $P(m) = (f/k_B T) \exp(-mf/k_B T)$, so the full distribution of r is given by

$$P_0(r) = \int_0^\infty dm P(m) P_0(r|m). \quad (29)$$

Evaluating this integral leads to the prediction summarized in Eq. (24). Similarly, the distribution $P_n(R)$ of $R(n)$ for any n can be obtained by summing over a conditional distribution, assuming that $m > n$ bases are open, and another one given that $m < n$ bases are open. The latter distribution is well approximated, except for n very near m , by the bulk distribution for dsDNA $P_\infty[R(n)]$ introduced earlier. Thus, we find that

$$\begin{aligned}
P_n(R) &= \int_n^\infty dm P(m) P_0(R|m-n) + P_\infty(R) \int_0^n dm P(m) \\
&= \exp\left(-\frac{nf}{k_B T}\right) P_0(R) + \frac{f}{k_B T} \left[1 - \exp\left(-\frac{nf}{k_B T}\right)\right] \\
&\quad \times P_\infty(R), \tag{30}
\end{aligned}$$

where $P_0(R|m-n)$ and $P_0(R)$ are given by Eqs. (28) and (29). Since $P_\infty(R)$ must be symmetric with respect to $R=0$, its average vanishes. Upon using Eq. (30) to evaluate $\langle R(n) \rangle$ and recalling that $f = |g_0| - 2g(F) = (F_c^2 - F^2)b^2/(k_B T)^2$ for a Gaussian chain, we recover Eqs. (26) and (27). Thus, the predictions obtained by studying directly the evolution equation (18) of the partition function coincide with those obtained by integrating out most degrees of freedom to arrive at a simplified formulation in terms of the unzipping energy $\mathcal{E}(m)$.

IV. DISORDER-AVERAGED BEHAVIOR

In contrast to the entropically driven opening of a homopolymer, the unzipping of a polymer with a random sequence is driven primarily by the possibility of lowering $\mathcal{E}(m)$ by unzipping a string of base pairs that are more weakly paired than the average. The two transitions are thus qualitatively different. To see this explicitly, consider a simple application of the Harris criterion for the importance of disorder [43]. The typical variation per monomer due to disorder in the base-pairing energy $\mathcal{E}(m)$ of a liberated section of length $\langle m \rangle$ is $(\Delta/\langle m \rangle)^{1/2} \sim \sqrt{F_c - F}$, where the F dependence follows from the result (17) for the divergence of $\langle m \rangle$ near the transition for a homopolymer. These energy variations vanish more slowly as $F \rightarrow F_c$ than the average energy difference $f \sim F_c - F$ between the two phases, indicating that sequence randomness dominates at the unzipping transition.

A related argument can help us to guess the correct critical exponent for the divergence of $\langle m \rangle$ when disorder is present: The contribution to $\mathcal{E}(m)$ of the average energy difference is mf , while a typical favorable contribution from random variations about the average is of order $-\sqrt{\Delta m}$. The random part thus exceeds the average for $m \lesssim m^* \equiv \Delta/f^2$. When this is the case, $\mathcal{E}(m)$ is roughly as likely to be negative as to be positive. One thus expects that a typical value of $\langle m \rangle$ will be at least of order m^* . Near enough to the unzipping transition at $f=0$, m^* is larger than the equilibrium average $k_B T/f$ for a nonrandom sequence. Instead of the $1/(F_c - F)$ divergence in $\langle m \rangle$ seen for a homopolymer, one might thus expect DNA with a random sequence to show a considerably stronger $1/(F_c - F)^2$ singularity. The crossover between the two scaling regimes should occur when $\Delta/f^2 \sim k_B T/f$, or when $f \sim \Delta/k_B T$. For dsDNA, both $\sqrt{\Delta}$ and the average base pairing energy g_0 are of order $k_B T$; we can estimate $f \approx g'(F_c)(F_c - F) \approx (g_0/F_c)(F_c - F)$. Hence, when $fk_B T/\Delta \sim O(1)$ at the crossover, the reduced force $(F_c - F)/F_c$ is also $O(1)$, confirming that disorder cannot be neglected in polynucleotide unzipping even for F of order, say, $F_c/2$. As we shall see in Sec. VII, disorder affects the

dynamics of unzipping for a similar range above F_c .

This scaling argument can be extended to the case of random DNA sequences with long-ranged correlations (as may be the case for noncoding DNA [6]). If the correlations between nucleotides separated by m base pairs decay as $1/m^\gamma$, the fluctuation $\eta(m)$ around the average energy to open a base pair will likewise have a correlation function $\overline{\eta(m)\eta(m')} \sim 1/|m-m'|^\gamma$. For $\gamma < 1$, the mean-squared value of $\int_0^m dm' \eta(m')$ then grows as $\int_0^m dm' \int_0^m dm'' 1/|m' - m''|^\gamma \sim m^{2-\gamma}$. A typical random contribution to $\mathcal{E}(m)$ then increases as $m^{1-\gamma/2}$, balancing this random energy against mf suggests that $\overline{\langle m \rangle} \sim m^* \sim f^{-2/\gamma}$. If we take, for example, $\gamma = \frac{2}{3}$ [6], then $\overline{\langle m \rangle} \sim 1/f^3$, an even stronger divergence.

To verify our scaling argument for the case of a random, uncorrelated base sequence, we begin by calculating the disorder-averaged number of bases opened $\overline{\langle m \rangle}$ (as before, the overbar indicates an average over different random base sequences). Fluctuations about this average will be studied in more detail in the following section. To find $\overline{\langle m \rangle}$, one must first compute the average free energy $-k_B T \ln Z$; disorder-averaged cumulants of m can then be obtained by taking derivatives with respect to f . Remarkably, the entire distribution of Z can be found exactly by treating the random energy η as a Langevin noise. Several variations on this procedure have appeared in other physical contexts [44], as have related approaches to the same formal problem [45].

We begin by defining the partition function of a polymer of finite length m ,

$$\tilde{Z}(m) = \int_0^m dm' \exp\left[-\frac{\mathcal{E}(m')}{k_B T}\right]. \tag{31}$$

The partition function Z of interest to us is recovered by taking the limit of an infinite length polymer: $Z = \lim_{m \rightarrow \infty} \tilde{Z}(m)$. The derivative of \tilde{Z} is simply

$$\frac{d\tilde{Z}}{dm} = e^{-\mathcal{E}(m)/k_B T}, \tag{32}$$

with initial condition $\tilde{Z}(0) = 0$. Similarly, the derivative of $\mathcal{E}(m)$ is, from Eq. (13),

$$\frac{d\mathcal{E}}{dm} = f + \eta(m), \tag{33}$$

with initial condition $\mathcal{E}(0) = 0$. Equations (32) and (33) make up a system of coupled Langevin equations, analogous, for example, to those describing the Brownian motion of a massive particle, with \mathcal{E} playing the role of momentum and \tilde{Z} that of position. They can be transformed in the usual manner into an equivalent Fokker-Planck equation for the joint probability distribution $P(\mathcal{E}, \tilde{Z}, m)$ of \mathcal{E} and \tilde{Z} at ‘‘time’’ m [46],

$$\frac{\partial P}{\partial m} = \left[\frac{\Delta}{2} \frac{\partial^2}{\partial \mathcal{E}^2} - f \frac{\partial}{\partial \mathcal{E}} - e^{-\mathcal{E}/k_B T} \frac{\partial}{\partial \tilde{Z}} \right] P. \tag{34}$$

To solve Eq. (34) in the limit of large m , we first Laplace transform with respect to \tilde{Z} and to m , with conjugate variables λ and s , respectively. The resulting ordinary differential equation for the transformed distribution $\hat{P}(\mathcal{E};\lambda,s)$ takes the form

$$\frac{\Delta}{2} \frac{d^2 \hat{P}}{d\mathcal{E}^2} - f \frac{d\hat{P}}{d\mathcal{E}} - \lambda e^{-\mathcal{E}/k_B T} \hat{P} - s \hat{P} = -\delta(\mathcal{E}). \quad (35)$$

The change of variables

$$x \equiv k_B T \left(\frac{8\lambda}{\Delta} \right)^{1/2} e^{-\mathcal{E}/(2k_B T)} \quad (36)$$

leads to an inhomogeneous Bessel equation

$$\begin{aligned} x^2 \frac{\partial^2 \hat{P}}{\partial x^2} + \left(1 + \frac{4fk_B T}{\Delta} \right) x \frac{\partial \hat{P}}{\partial x} - \left[x^2 + \frac{8s(k_B T)^2}{\Delta} \right] \hat{P} \\ = -\frac{4x_0 k_B T}{\Delta} \delta(x - x_0), \end{aligned} \quad (37)$$

where $x_0 \equiv x|_{\mathcal{E}=0} = k_B T \sqrt{8\lambda/\Delta}$. Although \mathcal{E} has been replaced by x , \hat{P} remains normalized as a function of \mathcal{E} . One can easily check that the solution of Eq. (37) follows the usual form for the Green's function of a Sturm-Liouville equation,

$$\hat{P}(x;\lambda,s) = k_B T \begin{cases} \frac{4}{\Delta} \left(\frac{x_0}{x} \right)^{2fk_B T/\Delta} K_\nu(x_0) I_\nu(x), & x \leq x_0 \\ \frac{4}{\Delta} \left(\frac{x_0}{x} \right)^{2fk_B T/\Delta} I_\nu(x_0) K_\nu(x), & x \geq x_0, \end{cases} \quad (38)$$

where I_ν and K_ν are modified Bessel functions, and

$$\nu = k_B T \sqrt{\frac{8s}{\Delta} + \frac{4f^2}{\Delta^2}}. \quad (39)$$

Equation (38) represents an exact solution to our single degree of freedom model. We are interested primarily in the distribution of \tilde{Z} for large m , so we would like to integrate over all \mathcal{E} and then take the limit $m \rightarrow \infty$. The first task can easily be accomplished on a formal level:

$$\begin{aligned} \hat{P}(\lambda,s) &= \int_{-\infty}^{\infty} d\mathcal{E} \hat{P}(\mathcal{E};\lambda,s) \\ &= \frac{8(k_B T)^2}{\Delta} \left[K_\nu(x_0) \int_0^{x_0} \frac{dx}{x} \left(\frac{x_0}{x} \right)^{2fk_B T/\Delta} I_\nu(x) \right. \\ &\quad \left. + I_\nu(x_0) \int_{x_0}^{\infty} \frac{dx}{x} \left(\frac{x_0}{x} \right)^{2fk_B T/\Delta} K_\nu(x) \right]. \end{aligned} \quad (40)$$

Because $\mathcal{E}(m)$ grows linearly with m below the unzipping transition for large enough m , the contributions to the partition function Z of the parts of the dsDNA at very large m are

exponentially suppressed. Hence, we expect that \tilde{Z} must have a well-defined limiting distribution as $m \rightarrow \infty$. This, in turn, implies that the Laplace transform $\hat{P}(\lambda,s)$ should diverge like $1/s$ as $s \rightarrow 0$, or equivalently, as $\nu \rightarrow 2fk_B T/\Delta$. An examination of Eq. (40) reveals that this is in fact the case. Specifically, $I_\nu(x) \sim x^\nu$ for small x , so the integral from 0 to x_0 diverges when ν approaches $2fk_B T/\Delta$. This singularity dominates the large m behavior of the inverse Laplace transform with respect to s , allowing us to perform the inversion analytically:

$$\begin{aligned} \hat{P}(\lambda; m \rightarrow \infty) &= \frac{2}{\Gamma(2fk_B T/\Delta)} \left[\frac{2\lambda(k_B T)^2}{\Delta} \right]^{fk_B T/\Delta} \\ &\quad \times K_{2fk_B T/\Delta} \left(k_B T \sqrt{\frac{8\lambda}{\Delta}} \right), \end{aligned} \quad (41)$$

where we have substituted $x_0 = k_B T \sqrt{8\lambda/\Delta}$. Note that the asymptotics are completely determined by the small x behavior of $\hat{P}(x;\lambda,s)$. Because small x corresponds to large \mathcal{E} , this is quite reasonable: It follows directly from Eq. (33) that the distribution of $\mathcal{E}(m)$ is a Gaussian centered at mf , so only very large \mathcal{E} will have any weight for large m .

To evaluate the disorder-averaged free energy, we must invert the Laplace transform $\hat{P}(\lambda; m \rightarrow \infty)$ to obtain the distribution $P(Z)$ of the partition function. With the aid of various Bessel function identities, one discovers that the integral can be evaluated analytically. The result is the distribution over possible random sequences of the partition function Z of our minimal unzipping model [44]:

$$\begin{aligned} P(Z) &= \frac{1}{\Gamma(2fk_B T/\Delta)} \left[\frac{2(k_B T)^2}{\Delta} \right]^{2fk_B T/\Delta} \left(\frac{1}{Z} \right)^{1+2fk_B T/\Delta} \\ &\quad \times \exp \left[\frac{-2(k_B T)^2}{Z\Delta} \right]. \end{aligned} \quad (42)$$

The disorder-averaged free energy follows immediately by integration; with the substitution $y \equiv 2(k_B T)^2/(Z\Delta)$, one has

$$\begin{aligned} -k_B T \overline{\ln Z} &= k_B T \left\{ \frac{1}{\Gamma(2fk_B T/\Delta)} \int_0^\infty dy y^{2fk_B T/\Delta - 1} \ln(y) e^{-y} \right. \\ &\quad \left. + \ln \left[\frac{\Delta}{2(k_B T)^2} \right] \right\}. \end{aligned} \quad (43)$$

Taking a derivative with respect to f yields the main quantity of interest,

$$\begin{aligned} \overline{\langle m \rangle} &= -k_B T \frac{\partial \overline{\ln Z}}{\partial f} \\ &= \frac{2(k_B T)^2}{\Gamma(2fk_B T/\Delta) \Delta} \int_0^\infty dy y^{2fk_B T/\Delta - 1} (\ln y)^2 e^{-y} \\ &\quad - \frac{2(k_B T)^2 \Gamma'(2fk_B T/\Delta)^2}{\Gamma(2fk_B T/\Delta)^2 \Delta}, \end{aligned} \quad (44)$$

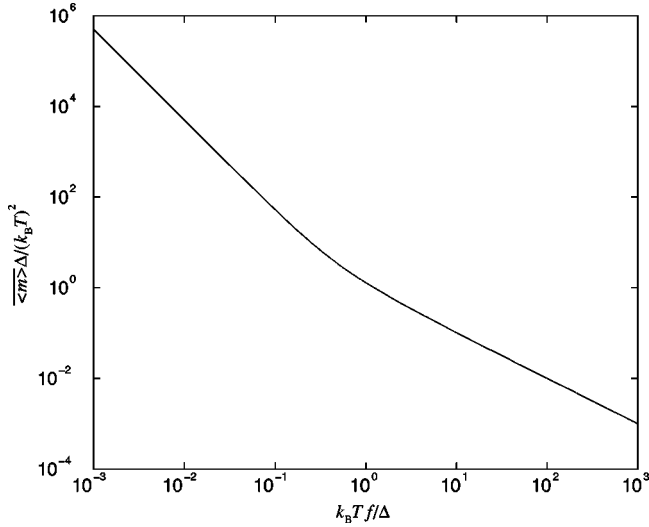


FIG. 7. Log-log plot of Eq. (44) for $\overline{\langle m \rangle}$ as a function of $f = 2g(F) - g_0 \sim F_c - F$. For large f , the plot has slope -1 , but it crosses over to slope -2 at $f \approx \Delta/k_B T$.

where $\Gamma'(z) = d\Gamma/dz$. This function is plotted in Fig. 7. In agreement with our earlier scaling argument, there is a cross-over from $1/f$ to $1/f^2$ behavior at f of order $\Delta/k_B T$. Indeed, one can analytically extract the asymptotic small f behavior from Eq. (44). One finds that to leading order as $f \rightarrow 0$,

$$\overline{\langle m \rangle} \approx \frac{\Delta}{2f^2} \sim \frac{1}{(F_c - F)^2} \quad (\text{random heteropolymer}). \quad (45)$$

Additional results follow for the higher cumulants of m . For example, the disorder-averaged variance of m can be found from the second derivative of $\ln Z$. For small f , $\overline{\langle m^2 \rangle} - \overline{\langle m \rangle}^2 = k_B T \partial^2 \ln Z / \partial f^2 \sim 1/f^3$. The square root of this variance is a length scale that can be compared to $\overline{\langle m \rangle}$. In the nonrandom case, both quantities are of order $k_B T/f$. In contrast, once sequence randomness is added, we have that $(\overline{\langle m^2 \rangle} - \overline{\langle m \rangle}^2)^{1/2} \sim 1/f^{3/2}$, which is much smaller than $\overline{\langle m \rangle}$ for sufficiently small f . Thermal fluctuations about $\overline{\langle m \rangle}$ in a given random heteropolymer thus become small compared to the mean near the transition. As we shall see in the following section, this fact allows us to predict not just disorder-averaged quantities (it might be tedious to average over all possible sequences in a real experiment), but also the unzipping behavior of a *single* dsDNA molecule.

V. FORCE-DISPLACEMENT CURVE FOR A SINGLE POLYNUCLEOTIDE DUPLEX

Figure 8 plots the average number of unzipped bases $\langle m \rangle$ versus force near the unzipping transition for simulations of four different dsDNA molecules, with different random sequences [47]. The corresponding energy landscapes for a force close to F_c are shown in Fig. 9. Far from being smooth, each $\langle m \rangle$ versus f curve shows long plateaus, where $\langle m \rangle$ remains essentially constant, separated by sudden, large jumps. The smoothly diverging precursor to the phase tran-

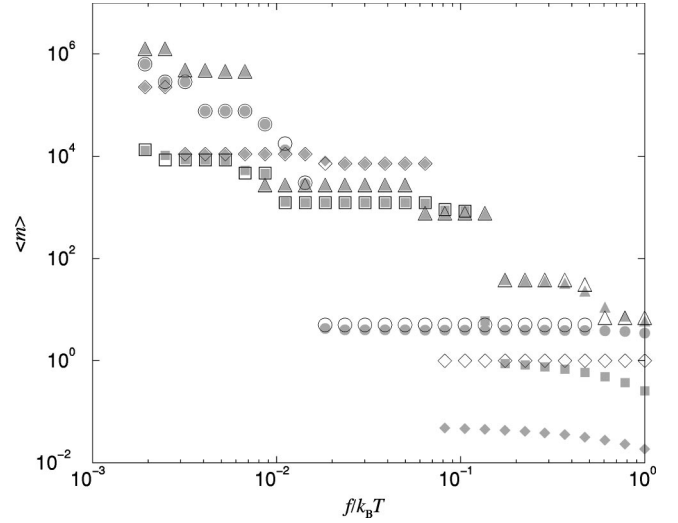


FIG. 8. Log-log plot of the average number of bases opened $\langle m \rangle$ (closed symbols) and the location of the absolute minimum m_{\min} of $\mathcal{E}(m)$ (open symbols) as a function of the distance f from the unzipping transition. Both variables are plotted for each of four individual polymers, represented by four different symbol shapes, with independently chosen random sequences [variance $\Delta = 9(k_B T)^2$] of length $N = 5 \times 10^6$ bases. Note that, except when $m = O(1)$, $\langle m \rangle$ and m_{\min} coincide very well. The energy landscapes for the four duplexes are plotted for a particular value of f in Fig. 9.

sition seen in homopolymers and in the disorder average $\overline{\langle m \rangle}$ has evidently been replaced by a series of “micro-first-order transitions.” The four traces, moreover, are not the same—the unzipping of a single random dsDNA does not exhibit self-averaging, but instead shows large sequence-dependent variations. Most equilibrium systems with quenched disorder are self-averaging because the macroscopic observables of interest are the sums of contributions from many essentially independent correlation volumes, each with their own independent realization of the quenched random variables; the central limit theorem then guarantees that in the thermodynamic limit, measurements will always coincide with the disorder average. In a single molecule DNA unzipping experiment, in contrast, one is probing only one realization of the quenched random sequence. As Fig. 9 indicates, each random realization of $\mathcal{E}(m)$ will be different, and the value of $\langle m \rangle$ at a given f can thus be expected to differ from one polymer to the next. Furthermore, for each sequence, $\mathcal{E}(m)$ varies over many tens of $k_B T$; one thus might expect that m would not fluctuate very far from the minima. Figure 8 bears out this idea: The location m_{\min} of the absolute minimum of $\mathcal{E}(m)$ for each value of f coincides remarkably well with $\langle m \rangle$. Because $\mathcal{E}(m)$ is usually negative at these minima, the dsDNA gains energy by unzipping some bases at its end, even below the bulk unzipping transition. This mechanism contrasts with the essentially entropic impetus for surface opening in the case of a homopolymer. We show in this section that, near enough to the transition, $\langle m \rangle$ for a given DNA or RNA duplex coincides with m_{\min} with arbitrary precision and that this fact can be used to gain a quantitative understanding of the abrupt jumps seen in Fig. 8. We will usually work in the continuum approximation, with the prob-

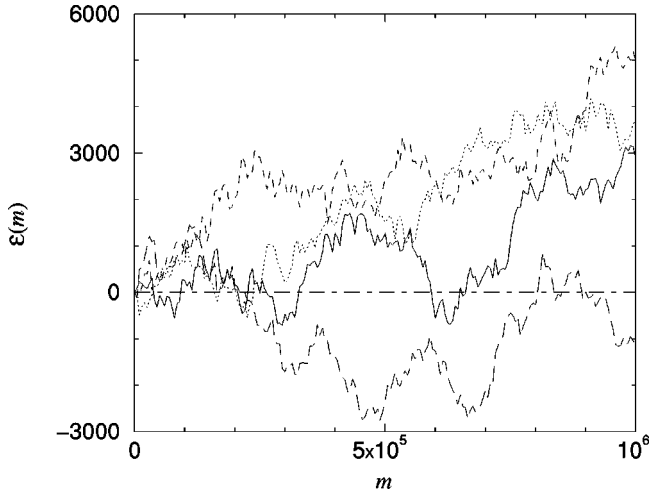


FIG. 9. Plot of four different random realizations of $\mathcal{E}(m)$. All four random walks have the same variance $\Delta = 9(k_B T)^2$ and average bias $f = 0.0025k_B T$. All four also pass below $\mathcal{E} = 0$, suggesting that, near the unzipping transition, dsDNA molecules with random sequences will usually have *energetic* reasons to partially unzip. The four energy landscapes are taken from the four polymers whose force-extension curves are shown in Fig. 8; the solid, dashed, dotted, and long-dashed curves correspond, respectively, to the circles, squares, diamonds, and triangles. In order to focus on regions where $\mathcal{E}(m)$ is near zero, the landscapes for $m > 10^6$ are not shown.

ability $P(\mathcal{E}, m)$ of finding an energy \mathcal{E} after opening m bases satisfying a diffusionlike equation,

$$\frac{\partial P}{\partial m} = \frac{\Delta}{2} \frac{\partial^2 P}{\partial \mathcal{E}^2} - f \frac{\partial P}{\partial \mathcal{E}}. \quad (46)$$

This result follows directly from Eq. (33) or from integrating the full Fokker-Planck equation (34) with respect to \bar{Z} . At each m , $\mathcal{E}(m)$ thus has a Gaussian distribution; because our results do not depend on the tails of this distribution, they should be equally valid for more realistic, discrete models of dsDNA.

A. Dominance of the absolute free energy minimum

We begin by arguing that, close to the transition, the location m_{\min} of the absolute minimum of $\mathcal{E}(m)$ is in fact the same as $\langle m \rangle$. More precisely, we wish to show that, for a random DNA sequence,

$$\lim_{f \rightarrow 0} \frac{\langle m \rangle}{m_{\min}} = 1 \quad \text{with probability 1.} \quad (47)$$

In qualitative terms, one might expect this result to hold because the scale of $\mathcal{E}(m)$ grows like the square root of the distance from the minimum; it is thus very unlikely that $\mathcal{E}(m)$ will revisit the neighborhood of its minimum value for m far from the location of the original minimum. Here, we simply outline the arguments necessary to support this intuition; closely related theorems have, however, been proven with mathematical rigor [48]. We will proceed by first con-

sidering scenarios in which Eq. (47) would not hold, then showing that the probability of each such event vanishes as $f \rightarrow 0$. In renormalization-group language, Eq. (47) can be read as stating that the unzipping transition for a random dsDNA sequence is governed by a zero-temperature fixed point; such fixed points have been found in a number of other random systems [49].

The simplest way that m_{\min} and $\langle m \rangle$ could differ is for m_{\min} to equal 0; since $\langle m \rangle$ is necessarily positive, their ratio would then be infinite. The probability that $m_{\min} = 0$ is the same as the probability that the biased random walk $\mathcal{E}(m)$, which starts at $\mathcal{E}(0) = 0$, has $\mathcal{E}(m) > 0$ for all $m > 0$. More generally, the probability that $\mathcal{E}(m) > 0$ for all $m > 0$ for a random walk starting at $\mathcal{E}(0) = \mathcal{E}_0$ is known in the literature on first passage problems as the “splitting probability” $\pi(\mathcal{E}_0)$. The splitting probability satisfies an equation involving the adjoint of the diffusion operator [46],

$$\frac{\Delta}{2} \frac{\partial^2 \pi}{\partial \mathcal{E}^2} + f \frac{\partial \pi}{\partial \mathcal{E}} = 0. \quad (48)$$

The solution of this equation with boundary conditions $\pi(0) = 0$ and $\pi(\infty) = 1$ is $\pi(\mathcal{E}_0) = 1 - \exp(-2\mathcal{E}_0 f / \Delta)$. The requirement that $\pi(0) = 0$ is an artifact of the behavior of a continuous time random walk as $m \rightarrow 0$: Because $\mathcal{E}(m)$ experiences small jumps up and down on all scales, a random walk that starts at $\mathcal{E}(0) = 0$ will pass below the line $\mathcal{E} = 0$ many times for very small m . This behavior is not relevant to real DNA with discrete bases, and we can regularize it by considering, instead of a random walk that starts exactly at $\mathcal{E}_0 = 0$, one that starts slightly above 0. For small \mathcal{E}_0 , $\pi(\mathcal{E}_0) \approx 2\mathcal{E}_0 f / \Delta$, so the splitting probability vanishes linearly as $f \rightarrow 0$. Indeed, for any \mathcal{E}_0 , $\pi(\mathcal{E}_0)$ goes to zero linearly for small f , as one might expect based on the well-known result that a completely unbiased random walk in one dimension must eventually visit the entire real line. The same linear behavior for small enough bias is seen in random walks on one-dimensional lattices [46]. We thus conclude that the probability that $m_{\min} = 0$ is proportional to f and can be neglected as $f \rightarrow 0$.

Now consider other possible values of m_{\min} . We shall see in the following section that the distribution of m_{\min} for $m_{\min} > 0$ is a function of the dimensionless ratio $m_{\min} f^2 / \Delta$. The probability that $m_{\min} \sim O(1/f^\beta)$, with $\beta \neq 2$, hence becomes negligible for small f , and we need only consider $m_{\min} \sim O(1/f^2)$. For the absolute minimum and the thermal average *not* to coincide in this case, there must be a local minimum nearly degenerate with $\mathcal{E}(m_{\min})$ a distance $O(1/f^2)$ away from m_{\min} . Note in particular that a degenerate minimum closer to m_{\min} than $O(1/f^2)$ will contribute an additive correction to $\langle m \rangle$ that is much smaller than $m_{\min} \sim O(1/f^2)$ for small enough f , and thus will not affect the ratio $\langle m \rangle / m_{\min}$ as $f \rightarrow 0$. The same holds true for thermal fluctuations in the well surrounding m_{\min} .

We can rephrase the question of the existence of degenerate minima as follows: What is the probability that, for a given positive E and ϵ ,

$$\mathcal{E}(m) > \mathcal{E}(m_{\min}) + E \quad \text{for all } m \text{ such that}$$

$$|m - m_{\min}| > \epsilon \Delta / f^2? \quad (49)$$

If this inequality is satisfied, then $\langle m \rangle / m_{\min} - 1$ is at most of the sum of a term of order ϵ and of a term of order $\exp(-E/k_B T)$; if for any choice of E and ϵ the probability that it is satisfied can be made arbitrarily close to 1 for f small enough, then Eq. (47) must hold. One can easily argue from dimensional analysis that this is the case: The probability $P_{\text{ineq.}}$ that the inequality Eq. (49) holds is a function of the dimensionless parameter ϵ and of the three parameters E , Δ , and f , with dimensions, respectively, of energy, (energy)²/nucleotide, and energy/nucleotide. Because $P_{\text{ineq.}}$ is itself dimensionless, it must depend only on dimensionless ratios of the latter three parameters; by rescaling energies and nucleotide numbers, one can easily conclude that the only such ratio is Ef/Δ . Hence, $P_{\text{ineq.}} = P_{\text{ineq.}}(\epsilon, Ef/\Delta)$. Moreover, we know that m_{\min} is the absolute minimum of the random walk, so it must be true that $P_{\text{ineq.}} = 1$ when $E = 0$. As long as $P_{\text{ineq.}}(\epsilon, Ef/\Delta)$ is a continuous function of its second argument, it must then be true that $P_{\text{ineq.}} \rightarrow 1$ as $f \rightarrow 0$ for any fixed ϵ and E . This is sufficient to confirm that m_{\min} and $\langle m \rangle$ coincide with probability 1 for small f . If $P_{\text{ineq.}}$ has a well-defined first derivative, then $1 - P_{\text{ineq.}} \sim Ef/\Delta$ for small f , a result that can be verified by a more detailed calculation.

This linear dependence has a simple interpretation: For an unbiased random walk, the probability to make a first return to the starting point after m steps decays as $1/m^{3/2}$; this is also approximately the case for a biased random walk on scales smaller than $\sim \Delta/f^2$. Upon integrating $1/m^{3/2}$ from $\epsilon \Delta/f^2$ to some large upper bound, we see that the probability not to return at all (and thus not to have any minima nearly degenerate with m_{\min}) differs from 1 by a number of order f . Our earlier observation that $\langle m^2 \rangle - \langle m \rangle^2 \sim 1/f^3$ can also be explained by the small f behavior of $1 - P_{\text{ineq.}}$ [44]: The disorder average is dominated by the probability of order f that $\langle m^2 \rangle - \langle m \rangle^2$ will be of order $1/f^4$. The notion that disorder averages of higher cumulants can be determined by rare configurations of the disorder in which there are two widely separated minima has been explored in several other random systems [49,50].

B. Statistics of minima: Plateaus and jumps

Having determined that the absolute minimum m_{\min} of $\mathcal{E}(m)$ and the average number $\langle m \rangle$ of bases opened coincide near the unzipping transition, we can now use this fact to study the $\langle m \rangle$ versus f curve for a *single* random sequence. Consider the effect on the energy landscape $\mathcal{E}(m)$ describing a given dsDNA molecule, with a given random sequence, of tuning the bias f towards zero. Decreasing f gradually tilts the energy landscape towards the horizontal, as illustrated in Fig. 10. The location of the absolute minimum will then remain constant over a range of f , giving rise to the observed plateaus. As the landscape tilts, however, local minima at larger values of m move downwards faster than those at smaller m . At certain specific values of f , the energy of a

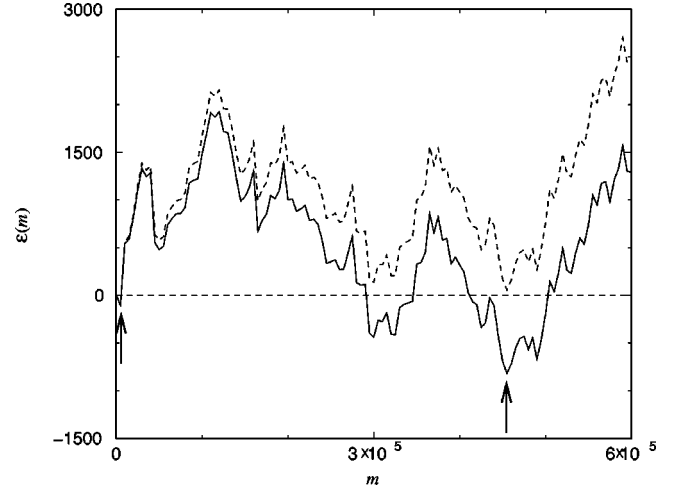


FIG. 10. Plot illustrating the physical origin of jumps in extension versus force during unzipping. The two curves represent random walks $\mathcal{E}(m)$ with identical random contributions $W(m)$, but different average biases $f_1 = 0.0087$ (upper curve) and $f_2 = 0.0067$ (lower curve). As indicated by the arrows, in the upper curve, the absolute minimum m_{\min} is at $m_{\min} \approx 5\,000$, while in the lower curve, it is at $m_{\min} \approx 445\,000$. As f is tuned from f_1 down to f_2 , m_{\min} and thus $\langle m \rangle$ jump from one minimum to the other.

minimum at $m > m_{\min}$ will move below $\mathcal{E}(m_{\min})$, and $m_{\min} \approx \langle m \rangle$ will shift from the old minimum to the new one. As Fig. 10 shows, the two minima can be separated by a considerable distance, thus giving a physical explanation for the dramatic jumps seen in Fig. 8.

To develop a quantitative theory of these effects, we begin by calculating the distribution of m_{\min} for a given f , then consider the conditional probability that $m_{\min} = m_2$ when $f = f_2$, given that the minimum was at m_1 at a bias f_1 . This conditional distribution will allow us to make predictions, for example, about the typical sizes of plateaus and jumps.

We first ask for the probability $P_{\min}(m_{\min}, \mathcal{E}_{\min})$ that $\mathcal{E}(m)$ has its absolute minimum at $(m_{\min}, \mathcal{E}_{\min})$, or equivalently the probability that $\mathcal{E}(m)$ first reaches \mathcal{E}_{\min} at “time” m_{\min} , multiplied by the probability that $\mathcal{E}(m) > \mathcal{E}_{\min}$ for $m > m_{\min}$. The latter is simply the splitting probability π introduced in the preceding subsection. Although in the continuum approximation $\pi(\mathcal{E}_0)$ is singular as $\mathcal{E}_0 \rightarrow \mathcal{E}_{\min}$, we can regularize it in a manner similar to that used previously. Because π is just a constant factor, independent of \mathcal{E}_{\min} , the details of the regularization are unimportant. In practice, π can be determined by demanding that $P_{\min}(\mathcal{E}_{\min}, m_{\min})$ be correctly normalized.

More interesting is the probability of first passage to \mathcal{E}_{\min} . We first define the probability $S(\mathcal{E}, m; \mathcal{E}_{\min})$ that, starting from $\mathcal{E} = 0$ at $m = 0$, the random walk has arrived at energy \mathcal{E} after opening m bases, without ever having had $\mathcal{E}(m) < \mathcal{E}_{\min}$. It turns out that S satisfies the same Fokker-Planck equation (46) as the probability $P(\mathcal{E}, m)$ for the unconstrained random walk to arrive at (m, \mathcal{E}) [46]. The constrained probability S , however, is also subject to the boundary condition $S(\mathcal{E}_{\min}, m; \mathcal{E}_{\min}) = 0$. With this boundary condition, one can solve the Fokker-Planck equation to find

$$S(\mathcal{E}, m; \mathcal{E}_{\min}) = \frac{1}{\sqrt{2\pi\Delta m}} \left\{ \exp\left[-\frac{(\mathcal{E}-fm)^2}{2\Delta m}\right] - \exp\left[\frac{f\mathcal{E}}{\Delta} - \frac{f^2 m}{2\Delta} - \frac{(2\mathcal{E}_{\min}-\mathcal{E})^2}{2\Delta m}\right] \right\}. \quad (50)$$

The probability to first cross \mathcal{E}_{\min} after m_{\min} steps is then given by $(\Delta/2)\partial S/\partial \mathcal{E}|_{\mathcal{E}=\mathcal{E}_{\min}}$, i.e., the diffusive flux of random walkers crossing \mathcal{E}_{\min} for the first time. The distribution $P_{\min}(\mathcal{E}_{\min}, m_{\min})$ differs from this function only by a normalization factor. Finally, we determine the probability that the minimum occurs at m_{\min} for any \mathcal{E}_{\min} by integrating from $-\infty$ to 0 with respect to \mathcal{E}_{\min} . The final result is

$$P_{\min}(m_{\min}) = \frac{f^2}{\pi\Delta} e^{-m_{\min}f^2/2\Delta} \int_0^{\infty} dw \times \exp(-wm_{\min}f^2/2\Delta) \frac{\sqrt{w}}{w+1}, \quad (51)$$

in agreement with the distribution obtained by le Doussal *et al.* using a real space renormalization group [50]. Note from Fig. 11 that $P_{\min}(m_{\min})$ agrees (within counting errors) with the distribution of $\langle m \rangle$ obtained from simulations. As claimed above, $P(m_{\min})$ takes the form of a scaling function of $m_{\min}f^2/\Delta$. Variations in $m_{\min} \approx \langle m \rangle$ between different random sequences are thus of the same order as the average $\langle m \rangle$, and the system is not self-averaging.

We now turn our attention to the more interesting and experimentally relevant question of correlations within a single $\langle m \rangle$ versus f curve. In particular, we would like to know the probability that $\mathcal{E}(m)$ has its minimum at m_2 at a bias f_2 given that, for the *same* realization $\eta(m)$ of the random base sequence, the minimum was at m_1 at a bias $f_1 > f_2$. This probability will turn out to depend only on the jump size $m_{\text{jump}} \equiv m_2 - m_1$. The plateaus seen in Fig. 8 suggest a δ function contribution at $m_{\text{jump}} = 0$. To determine the strength of this δ function, consider a polymer with a fixed base sequence giving rise to an energy landscape

$$W(m) \equiv \int_0^m dm' \eta(m'). \quad (52)$$

If the minimum of $\mathcal{E}(m)$ is at m_1 for bias f_1 , then $W(m) + f_1 m > W(m_1) + f_1 m_1 \equiv \mathcal{E}_1$ for all m , and hence $W(m) + f_2 m > W(m_1) + f_2 m_1 \equiv \mathcal{E}_2$ for $m < m_1$ and $f_2 < f_1$. If the minimum is to move from m_1 as the bias is tuned down to f_2 , it must move towards larger m . This is not surprising—one can easily prove that $d\langle m \rangle/df < 0$.

Let Π_1 and Π_2 denote the events, respectively, that for $m > m_1$, $W(m) + f_1 m > \mathcal{E}_1$, and $W(m) + f_2 m > \mathcal{E}_2$. The probabilities that Π_1 and Π_2 occur are simply the splitting probabilities $\pi_1 \propto f_1$ and $\pi_2 \propto f_2$. If the minimum of the random walk falls at m_1 for a bias f_1 , then Π_2 is true if and only if the minimum remains at m_1 at the bias f_2 . In other words, the coefficient of the δ function at $m_{\text{jump}} = 0$ in the distribution of m_{jump} is simply the conditional probability $\text{Prob}[\Pi_2|\Pi_1]$. From Bayes' theorem [51], we know that the

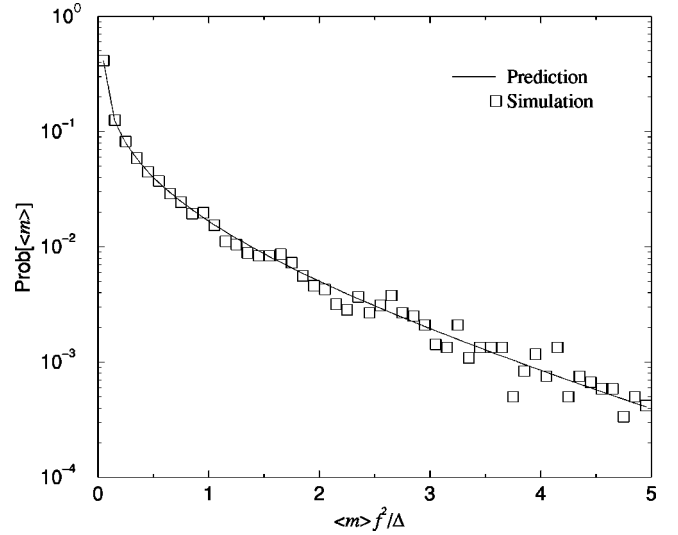


FIG. 11. Log-linear plot of the distribution over different random sequences of the average number of opened bases $\langle m \rangle$. The horizontal axis gives $\langle m \rangle$, suitably rescaled so that random sequences with different values of f and Δ can be compared. The vertical axis shows the log of the probability of seeing a particular $\langle m \rangle$. The squares represent binned data from numerical simulations (described in the Appendix), the solid curve the analytic prediction of Eq. (51) based on the assumption that $\langle m \rangle = m_{\min}$. This prediction has no adjustable parameters. The scatter seen for large $\langle m \rangle f^2 / \Delta$ is the result of counting noise.

probability that events Π_1 and Π_2 both occur for the same random sequence is $\text{Prob}[\Pi_2 \wedge \Pi_1] = \text{Prob}[\Pi_2|\Pi_1]\text{Prob}[\Pi_1]$. But if Π_2 occurs, then Π_1 must also occur—if the random walk never passes below its value at m_1 with the smaller bias f_2 , then it can never do so with the larger bias f_1 . Thus, $\text{Prob}[\Pi_2 \wedge \Pi_1] = \text{Prob}[\Pi_2]$. The conditional probability thus takes the simple form

$$\text{Prob}[\Pi_2|\Pi_1] = \frac{\text{Prob}[\Pi_2]}{\text{Prob}[\Pi_1]} = \frac{\pi_2}{\pi_1} = \frac{f_2}{f_1}, \quad (53)$$

and the probability that a plateau stretches from f_1 down to f_2 is just f_2/f_1 . Upon taking a derivative with respect to f_2 , we conclude that the end point of a plateau that starts at a bias f_{start} is uniformly distributed between 0 and f_{start} . Equivalently, the log ratio $l \equiv \ln(f_{\text{start}}/f_{\text{stop}})$ of the starting and ending biases of a plateau is distributed as $\exp(-l)$.

The distribution of plateau lengths, of course, is only part of the description of a plot of $\langle m \rangle$ versus f ; to complete the characterization, we must also study the distribution P_{jump} of jumps m_{jump} for nonzero m_{jump} . The full distribution of m_{jump} will then take the form $(f_2/f_1)\delta(m_{\text{jump}}) + (1 - f_2/f_1)P_{\text{jump}}(m_{\text{jump}})$. The calculation of P_{jump} requires an extension of our previous first passage approach. As before, we are interested in the probability that the biased random walk $W(m) + f_2 m$ first reaches the energy \mathcal{E}_2 at $m_2 = m_1 + m_{\text{jump}}$, but subject now to the additional constraint that (m_1, \mathcal{E}_1) is the absolute minimum for the larger bias f_1 . Hence, we demand that $W(m) + f_1 m > \mathcal{E}_1$ for all $m > m_1$, where $W(m)$ is the same fixed realization of the random

energy landscape. To calculate this modified first passage probability, note that for each m , only one of the two conditions has to be taken into account. For $m_{\text{jump}} < (\mathcal{E}_1 - \mathcal{E}_2)/(f_1 - f_2)$, $W(m) + f_1 m > \mathcal{E}_1$ is the stronger constraint on the allowed value of $\mathcal{E}(m)$, while for $m_{\text{jump}} > (\mathcal{E}_1 - \mathcal{E}_2)/(f_1 - f_2)$, $W(m) + f_2 m > \mathcal{E}_2$ is the stronger. We can find the first passage probability, subject to both constraints, by multiplying the probability of arriving at $m_{\text{jump}} = (\mathcal{E}_1 - \mathcal{E}_2)/(f_1 - f_2)$ subject to the first constraint by the probability of going from there to (m_2, \mathcal{E}_2) subject to the second. Specifically, let $S_1(\mathcal{E}, m; \mathcal{E}_{\min})$ be the probability of arriving at \mathcal{E} after opening m bases, with bias f_1 and with $\mathcal{E}(m)$ always larger than \mathcal{E}_{\min} , and let $S_2(\mathcal{E}, m; \mathcal{E}_{\min})$ be the corresponding probability with bias f_2 . Both probabilities are given by Eq. (50), with the appropriate substitution for f . As in our calculation of the distribution of minima, the derivative of S is also an important quantity, so it is useful to define $S'_{1,2}(\mathcal{E}, m; \mathcal{E}_{\min}) \equiv \partial S_{1,2}/\partial \mathcal{E}$. The probability that a random walk with bias f_2 will arrive at (m, \mathcal{E}) , subject to the constraint that $W(m) + f_1 m > \mathcal{E}_1$, is related to S_1 by a ‘‘Galilean’’ transformation (with m viewed as a time and $f_1 - f_2$ viewed as a velocity jump). Upon making use of the invariance of the S 's with respect to uniform translations in \mathcal{E} and in m , one can thus write the probability that (m_2, \mathcal{E}_2) is the minimum at bias f_2 , given that (m_1, \mathcal{E}_1) is the minimum at bias f_1 , as

$$P_{\text{jump}}(\mathcal{E}_2, m_2 | \mathcal{E}_1, m_1) \propto \int_{\mathcal{E}_2}^{\infty} d\mathcal{E}' S_1[\mathcal{E}' - \mathcal{E}_1 + (f_1 - f_2) \\ \times (m' + m_1), m'; 0] S_2'(\mathcal{E}_2 - \mathcal{E}', m_2 \\ - m_1 - m'; \mathcal{E}_2 - \mathcal{E}'), \quad (54)$$

where $m' \equiv (\mathcal{E}_1 - \mathcal{E}_2)/(f_1 - f_2)$ is the value of $m_{\text{jump}} \equiv m_2 - m_1$ at which the two constraints switch precedence. The quantity $S_1[\mathcal{E}' - \mathcal{E}_1 + (f_1 - f_2)m', m'; 0]$, which is formally zero, is assumed to be regularized by replacing 0 by $-\epsilon$, and we have suppressed the normalization factor proportional to π_2 . According to Eq. (54), P_{jump} depends only on the two biases f_1 and f_2 and on the differences m_{jump} and $\mathcal{E}_{\text{jump}} \equiv \mathcal{E}_2 - \mathcal{E}_1 + (f_1 - f_2)m_1$. The latter is the difference between $\mathcal{E}(m_1)$ and $\mathcal{E}(m_2)$, both defined with bias f_2 ; the extra factor proportional to m_1 is necessary because \mathcal{E}_1 is defined with bias f_1 . It is straightforward to show that the conditional distributions of minima are Markovian—that is, the joint distribution of m_2 and \mathcal{E}_2 does not depend on the location of the absolute minimum for any $f < f_1$: Suppose that one were to ask for the distribution of m_2 and \mathcal{E}_2 subject not only to the constraint that at bias f_1 , the minimum was at (m_1, \mathcal{E}_1) , but also that at a bias $f_0 < f_1$, the minimum was at $m_0 < m_1$ and \mathcal{E}_0 , with $\mathcal{E}_1 + (f_0 - f_1)m_0 < \mathcal{E}_0 < \mathcal{E}_1 + (f_0 - f_1)m_1$. This additional demand translates into the condition that $W(m) + f_0 m > \mathcal{E}_0$ for $m > m_1$. This constraint, however, is weaker than the requirement $W(m) + f_1 m > \mathcal{E}_1$ imposed by the location of the minimum at the bias f_1 . The distribution of (m_2, \mathcal{E}_2) is thus independent of what happens at f_0 , and the probability of a given sequence of measurements of $\langle m \rangle = m_{\min}$ for successive values of f can be expressed as a product of factors of P_{jump} .

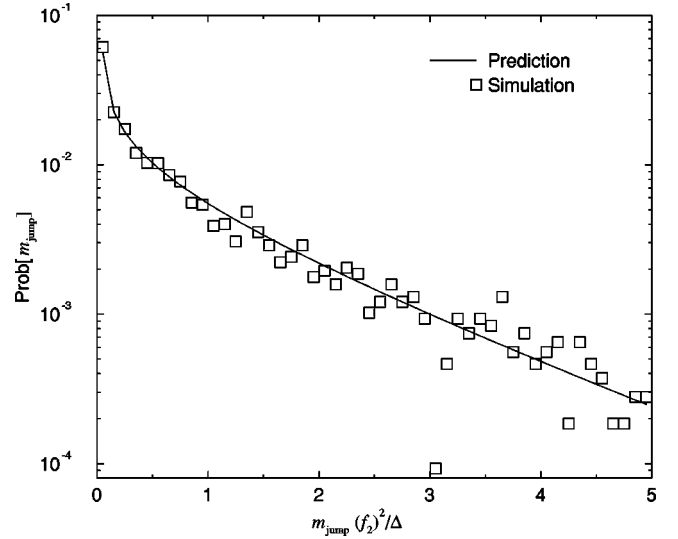


FIG. 12. Log-linear plot of the distribution of jumps m_{jump} for $f_2/f_1 \approx 0.77$. $m_{\text{jump}} f_2^2/\Delta$ is plotted on the horizontal axis, the log of the probability of m_{jump} on the vertical axis. The points represent binned data from numerical simulations (described in the Appendix), the solid curve an analytic prediction (no adjustable parameters) based on the assumption that $\langle m \rangle = m_{\min}$. The scatter seen for large $m_{\text{jump}} f_2^2/\Delta$ is the result of counting noise.

To find the distribution of m_{jump} alone, and thus of m_2 , one must integrate $P_{\text{jump}}(m_{\text{jump}}, \mathcal{E}_{\text{jump}})$ with respect to $\mathcal{E}_{\text{jump}}$ from $-(f_1 - f_2)m_2$ to 0. The lower bound reflects the constraint that $W(m_2) + f_1 m_2 > \mathcal{E}_1$; the upper bound ensures that $\mathcal{E}_2 < \mathcal{E}(m_1)$. Figure 12 compares a numerical calculation of the full distribution P_{jump} obtained in this way with simulation results. The good agreement confirms that $\langle m \rangle \approx m_{\min}$. The figure also shows that for large m_{jump} , P_{jump} decays as $\exp(-m_{\text{jump}} f_2^2/2\Delta)$. This is the same as the large m_{\min} behavior of P_{\min} with $f = f_2$; for large enough m_{jump} , the constraint imposed by the minimum at m_1 has no effect on the distribution.

Additional analytic insight can be obtained by considering various limits. When $(f_1 - f_2)/f_2 \gg 1$, one finds that $P_{\text{jump}}(m_{\text{jump}}, \mathcal{E}_{\text{jump}}) \approx P_{\min}(m_{\text{jump}}, \mathcal{E}_{\text{jump}})$, where P_{\min} is the distribution of the absolute minimum at a given value of f discussed above [Eq. (51)], evaluated with $f = f_2$. In the limit of large $f_1 - f_2$, the lower bound on $\mathcal{E}_{\text{jump}}$ approaches $-\infty$, and the integral of P_{jump} with respect to $\mathcal{E}_{\text{jump}}$ introduces no extra complications. The distribution of m_{jump} is thus no different from that of the minimum m_{\min} without any additional constraints. After normalization, we find

$$P_{\text{jump}}(m_{\text{jump}}) = P_{\min}(m_{\text{jump}}) = \frac{f^2}{\pi \Delta} \exp(-m_{\text{jump}} f^2/2\Delta) \\ \times \int_0^{\infty} dw \exp(-w m_{\text{jump}} f^2/2\Delta) \\ \times \frac{\sqrt{w}}{w+1} \left(\frac{f_1 - f_2}{f_2} \gg 1 \right). \quad (55)$$

Equation (55) can be understood as follows: When f_2 is much smaller than f_1 , the smaller bias allows the system to visit much more random sequence before the fm term in $\mathcal{E}(m)$ makes the energy cost prohibitive. With so many more places where the new absolute minimum could occur, the constraint from the location of the old minimum at the larger bias becomes unimportant, and $P_{\text{jump}}(m_{\text{jump}})$ becomes independent of m_1 . Indeed, because $m_2 \sim 1/f_2^2$ is typically much larger than $m_1 \sim 1/f_1^2$, m_2 differs very little from m_{jump} . The distribution of m_2 thus approaches $P_{\text{min}}(m_2)$. That is, the minimum at bias f_2 is essentially chosen *independently* from the same scaling distribution as the minimum at bias f_1 . With a long enough sequence, it should in principle be feasible to make many such independent measurements of $m_{\text{min}} \approx \langle m \rangle$ at different values of f . Although DNA unzipping is not self-averaging in the usual sense, the data from even a single random sequence thus nevertheless contain remnants of the disorder averaged behavior. In particular, if $\ln m$ is plotted versus $\ln f$ for a long enough polymer, the best-fit line should have slope -2 , as predicted by our calculation of the disorder-average $\langle \overline{m} \rangle$ [Eq. (45)], albeit with considerable scatter about the line. Figure 13 illustrates this point.

The distribution of m_{jump} in the opposite limit ($f_1 - f_2)/f_2 \ll 1$ is the size distribution of jumps between two successive plateaus, one ending and the other starting at $f_1 \approx f_2$. Put in different terms, it gives the distribution of distances between two essentially degenerate minima at a given bias f , assuming that such minima exist. Because the two minima are already required to be at almost the same energy, P_{jump} is independent of $\mathcal{E}_{\text{jump}}$ in this limit. The integral over $\mathcal{E}_{\text{jump}}$ is then elementary, and the resulting distribution takes the form

$$P_{\text{jump}}(m_{\text{jump}}) = \frac{f_2}{\sqrt{2\pi\Delta}} \frac{1}{\sqrt{m_{\text{jump}}}} \exp\left(-\frac{m_{\text{jump}}f_2^2}{2\Delta}\right) \times \left(\frac{f_1 - f_2}{f_2} \ll 1\right). \quad (56)$$

This expression is valid for $m_{\text{jump}}f_2^2/\Delta \lesssim f_2/(f_1 - f_2)$; for larger values of m_{jump} , the power law prefactor of P_{jump} crosses over from $1/(m_{\text{jump}})^{1/2}$ to $1/(m_{\text{jump}})^{3/2}$. The tail of the distribution thus still agrees with that of P_{min} , as expected.

Knowledge of P_{jump} gives a detailed description of the statistics of $\langle m \rangle$ versus f curves, under the assumption that $\langle m \rangle$ and m_{min} coincide. We have already seen that this assumption is valid with probability 1 as $f \rightarrow 0$. For any finite f , however, there will be occasions when it does not hold. In particular, it must break down in the vicinity of jumps between different plateaus. Near enough to a jump, the minima giving rise to the two plateaus will be nearly degenerate, and $\langle m \rangle$ will contain substantial contributions from both minima. Indeed, if a jump of size m_{jump} occurs at a bias f_1 , then both minima will be appreciably occupied if the difference between their energies $|f - f_1| m_{\text{jump}} \lesssim k_B T$. The sharp discontinuity in $\langle m \rangle$ at f_1 will be replaced by a smooth transition of width of order $k_B T / m_{\text{jump}}$. We have already seen that m_{jump} is typically of order Δ/f_1^2 , so the width of a typical transition

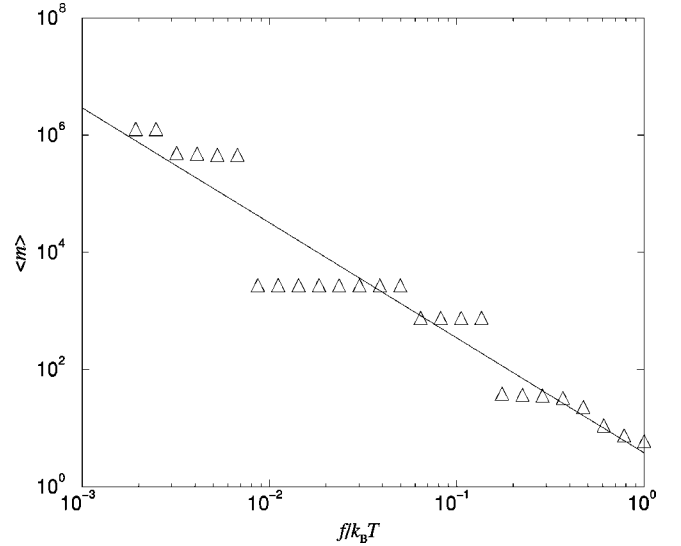


FIG. 13. Plot illustrating the recovery of the disorder-averaged scaling law $\langle m \rangle \approx \Delta/2f^2$ in the force-extension curve of a single random heteropolymer. The points give $\langle m \rangle$ as a function of f for a single polymer; the solid line is the best-fit power law, with exponent -1.96 ± 0.12 .

sharpens as f_1^2 . In contrast, we have seen that a typical plateau at bias f_1 extends for a distance of order f_1 . As $f_1 \rightarrow 0$, the width of the jumps thus becomes very small compared to the size of the plateaus, in agreement with our arguments that $m_{\text{min}}/\langle m \rangle \rightarrow 1$ in this limit. The sharpening of the jumps as $f \rightarrow 0^+$ is evident in Figs. 8 and 13.

Note also that if the temperature is raised at fixed force near the unzipping transition (i.e., a vertical instead of a horizontal trajectory in the inset to Fig. 1), we have $f \sim T_C - T$. The surface contribution to the specific heat near the transition is thus $T \partial^2 G / \partial T^2 \sim T^2 \partial \ln Z / \partial f^2 \sim \partial \langle m \rangle / \partial f$, where $G = -k_B T \ln Z$ is the “surface” free energy of the partially unraveled polymer duplex at fixed temperature and force defined in Sec. III. If $\langle m \rangle$ as a function of f takes the form of a sequence of plateaus and jumps, then the derivative of $\langle m \rangle$ with respect to f must vanish except in the vicinity of the jumps, where it will show a sharp spike proportional to the jump size m_{jump} . As $f \rightarrow 0$ and the jumps become very sharp, the specific-heat spikes will approach δ functions. Each jump can thus be thought of as a “micro-first-order transition.”

We close this section with an example of how plateaus and jumps can appear in the unzipping of a biologically relevant DNA sequence, that of phage lambda [52]. Figure 14 plots the energy landscape $\mathcal{E}(m)$ of a 28-kb segment of the lambda genome for two different biases. The energy to open each base pair is taken from a widely used parameter set [34], and we neglect the possibility of rare denaturation bubbles under physiological conditions. The energy landscape shows two pronounced minima; a third minimum very near $m=0$ is barely visible. The corresponding plot of $\langle m \rangle$ versus the distance $f \sim F_c - F$ from the transition, determined by an exact evaluation of the partition function, appears in Fig. 15. As expected, it consists of three plateaus, corresponding to the three minima. Thus, the qualitative ideas developed in this section apply to real sequences found in

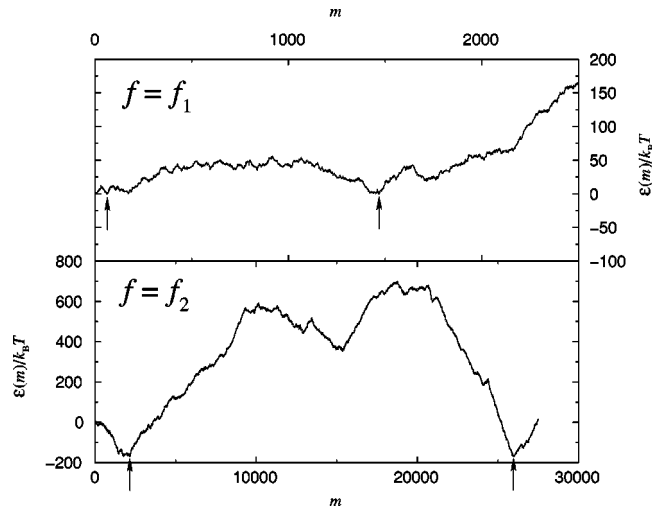


FIG. 14. The energy landscape $\mathcal{E}(m)$ for unzipping bacteriophage lambda DNA at two different biases. In this figure, the base pairs are opened in the reverse of the conventional [52] order, starting with base number 48 502. Base pairing and stacking energies are taken from [34] and are scaled by $k_B T$, with $T=37^\circ\text{C}=310\text{ K}$. The biases f_1 and f_2 are the locations of the two jumps marked in the force-extension curve of Fig. 15. The locations of the two minima that exchange stability at each bias are indicated by arrows. Note the difference in scales between the upper and lower plots.

experimental biology as well as to the idealized random models explored here.

C. Application: Determination of base-pairing energies

In this section, we digress briefly from our primary focus on polynucleotides with random sequences to discuss how the mechanical denaturation of specially designed sequences might be used to measure the strength of the base pairing and stacking interactions that stabilize polynucleotide duplexes. Traditionally, these interactions have been studied by analyzing the thermal melting curves of double-stranded DNA's and RNA's [34,58]. Most commonly, the stability of a duplex is assumed to be determined by ten phenomenological parameters giving the combined pairing and stacking energies of the ten possible distinct groups of two successive base pairs. These parameters can be inferred from the melting temperatures of a set of duplexes with appropriately chosen sequences. Although in most ways quite successful, this method has the disadvantage that it yields values of the ten energy parameters only in the vicinity of the melting temperatures of the double-stranded molecules. Because these energy parameters are expected to depend on a variety of conditions, including salt concentration, pH, and (for entropic reasons) temperature, it would be useful to have a technique that allowed the measurement of duplex stability in a wider range of conditions. It has already been shown experimentally that micromechanical experiments can be used to estimate the binding energy of a particular RNA hairpin [3]. Here we extend the analysis of Ref. [3] to consider more generally how mechanical denaturation might be used to infer the stability of duplexes.

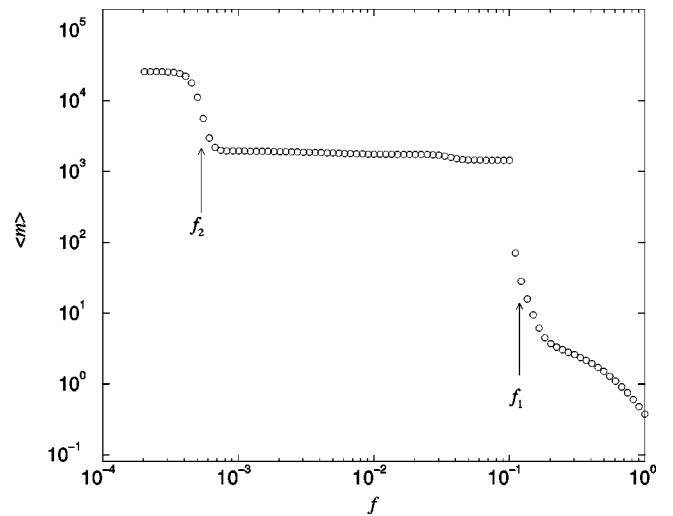


FIG. 15. Log-log plot of the average number of open bases $\langle m \rangle$ versus bias f for unzipping bacteriophage lambda DNA. The energy $\mathcal{E}(m)$ is as in Fig. 14. The three plateaus correspond to the minima of $\mathcal{E}(m)$ at $m \approx 1$, $m \approx 1500$, and $m \approx 26\,000$; the jumps between them occur at biases f_1 and f_2 as indicated in the figure. Assuming freely jointed chain elasticity for ssDNA [Eq. (7)], with $b=1.5\text{ nm}$ [33], the definition of f [Eq. (12)] implies that these biases correspond respectively to forces of $F_1=7.90\text{ pN}$ and $F_2=8.14\text{ pN}$. The middle plateau is actually subdivided into three smaller plateaus, separated by jumps between nearby minima. Similarly, a local minimum at $m=60$ is the most stable for a small range of f between the plateaus at $m=1$ and $m \approx 1500$.

Because it is difficult to synthesize long polynucleotides with prescribed sequences, one would like to be able to measure pairing energies on relatively short (tens of nucleotides) hairpins. Even for short hairpins, one can still define an average pairing energy g_0 , a variation about the average $\eta(m)$, a critical unzipping force F_c satisfying Eq. (16), and a distance $f=2g(F_c)-g_0$ from the transition. Drawing on the ideas developed in Secs. V A and V B, we expect that, for a given hairpin in the constant force ensemble, $\langle m \rangle$ will remain close to minima of $\mathcal{E}(m)$ except for jumps at certain values of f . The measurement of g_0 for a hairpin of length N is most straightforward if there are only two such minima, at $m=0$ and $m=N$; the unzipping transition then shows a two-state behavior [34]. For this to be the case, the energy landscape $\mathcal{E}(m)$ must take roughly the form shown in Fig. 16. Because of the energy barrier between $m=0$ and $m=N$, the unzipping fork is always localized in the vicinity of one of these minima, with a sharp jump between the two at F_c (Fig. 17). F_c is thus easily read off from the experimental extension versus force curve, and g_0 is then given by Eqs. (8) and (16). Just as for the standard methods based on melting curves, the ten energy parameters can be estimated from the knowledge of g_0 for enough different hairpins. One can straightforwardly design hairpins with two-state unzipping behavior by joining a stretch of strongly paired bases to a less stable stretch. Thus, for example, if one strand of the hairpin has sequence $5'(C)_{N/2}(A)_{N/2}3'$, with opening starting from the $5'$ end [and complementary sequence $3'(G)_{N/2}(T)_{N/2}5'$], g_0 for the hairpin approaches for large

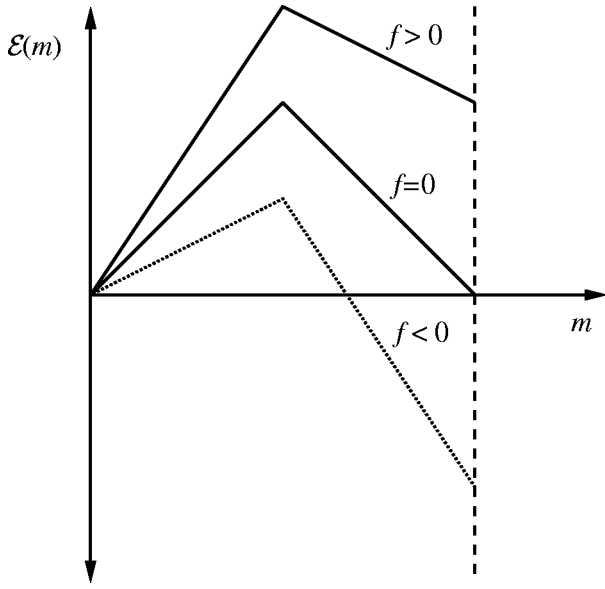


FIG. 16. Schematic energy landscape for a designed oligonucleotide duplex that could be used to measure base pairing and stacking energies. The duplex is chosen to have stronger base pairs near the end from which it is opened, and weaker base pairs at the far end. The energy of opening $\mathcal{E}(m)$ thus first slopes upwards, then downwards, and the only two minima occur for a completely unzipped and completely zipped ($m=0$) duplex. As the bias is tuned through the unzipping transition, the two minima exchange stability, giving rise to a sharp unzipping transition (see Fig. 17).

N , the average of the energies associated with (reading along one strand of a duplex) $5'CC3'$ and $5'AA3'$. Similarly, $5'(CG)_{N/4}(AT)_{N/4}3'$, paired with its complement, gives the average of the energies associated with $5'CG3'$, $5'GC3'$, $5'AT3'$, and $5'TA3'$. Corrections due both to the junction between the two homopolymeric stretches and to the confinement energy of the loop section of the hairpin decay as $1/N$; they can be eliminated by measuring hairpins with several different values of N . Mechanical denaturation in the constant force ensemble can thus be used systematically to determine the ten standard duplex stability parameters in a wide range of pH, salt concentration, and temperature.

VI. CONSTANT EXTENSION ENSEMBLE

So far, we have considered only the constant force ensemble, in which a fixed force is applied to the two single strands of the dsDNA, and one measures the average number of base pairs opened or the average separation $\langle \mathbf{r} \rangle$ between the ends of the two single strands. Constant extension experiments, in which the separation \mathbf{r} is fixed, and the average force is measured, are also possible. In the classical thermodynamics of macroscopic systems, these two ensembles would be equivalent. That is, the functions $\langle \mathbf{r} \rangle(\mathbf{F})$ and $\langle \mathbf{F} \rangle(\mathbf{r})$ measured in the two ensembles would be inverses of each other. In single molecule experiments, however, such a relation is not guaranteed, and the two ensembles are in fact not equivalent in DNA unzipping. For simplicity, we assume throughout this section that the Kuhn length b of the single-

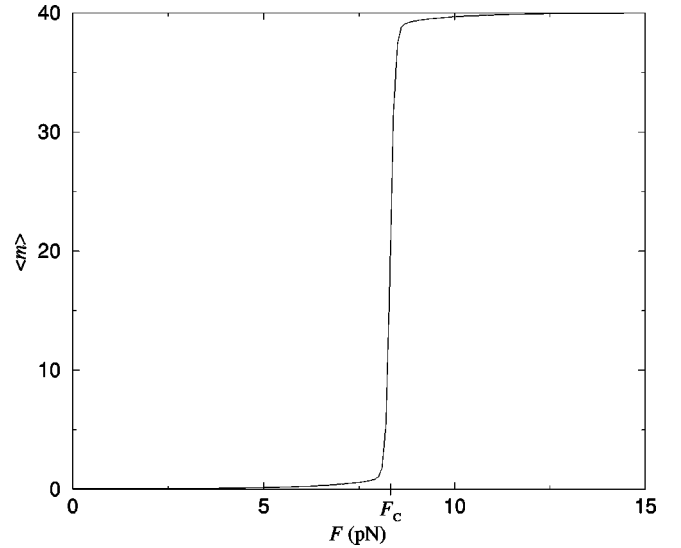


FIG. 17. Force extension plot for a designed oligonucleotide duplex that could be used to measure base pairing and stacking energies (see Fig. 16). Starting from the end from which it is being unzipped, the duplex has sequence $5'(A)_{20}(C)_{20}3'$, with base pairing energies taken from Ref. [34]. The sharp unzipping transition allows an accurate measurement of $F_c = 8.32$ pN, and thus of the energies stabilizing the duplex. Forces are calculated assuming that ssDNA is a freely jointed chain [Eq. (7)], with Kuhn length $b = 1.5$ nm [33].

stranded polymer is equal to the length a per chemical monomer.

We begin by considering the constant extension ensemble in the *absence* of sequence randomness. We neglect long-ranged interactions within the single-stranded polymers; because \mathbf{r} and \mathbf{F} will always be parallel on average, we can work with the (signed) scalars r and F . Regardless of the elastic properties of the single-stranded DNA (freely jointed chain, Gaussian, etc.), one can define the statistical weight $G_{2m}(r)$ for a single-stranded chain of length $2m$ to have an end-to-end distance r . The partition function \mathcal{Z} in the constant extension ensemble can then be viewed as a weighted sum over the number of unzipped bases m with r fixed. Given the energy cost $g_0 m$ of opening m bases, one has [19,21]

$$\mathcal{Z}(r) = \int_0^\infty dm G_{2m}(r) \exp(-g_0 m / k_B T). \quad (57)$$

In the limit of large r , one expects the number of unzipped bases m to be proportional to r . It then makes sense to consider the free energy per base $h(x)$ of the liberated single strands as a function of the extension per base $x \equiv r/2m$. The free energy per base $g(F)$ in the constant force ensemble is related to $h(x)$ by the Legendre transform $g(F) = h[x(F)] - Fx$, and in the thermodynamic limit $r \rightarrow \infty$ with r/m fixed, we expect $-k_B T \ln[G_{2m}(r)] \approx 2mh(x)$. It is not difficult to show that the leading correction to this result is of order $\ln(m)/2$. Hence, for large r the partition function becomes, up to r -independent multiplicative constants,

$$\begin{aligned}\mathcal{Z}(r) &\simeq \int_0^\infty \frac{dm}{m^{1/2}} \exp\left[-\frac{2m}{k_B T} h\left(\frac{r}{2m}\right) - \frac{g_0 m}{k_B T}\right] \\ &= \sqrt{\frac{r}{2}} \int_0^\infty \frac{dn}{n^{1/2}} \exp\left\{-\frac{r}{k_B T} \left[nh(1/n) - \frac{g_0 n}{2}\right]\right\},\end{aligned}\quad (58)$$

where we have introduced $n = 2m/r = 1/x$ in the second line. For large r , \mathcal{Z} may be evaluated in the saddle point approximation, which gives

$$\mathcal{Z}(r) \simeq \sqrt{\frac{(n^*)^2 \pi}{h''(1/n^*)}} \exp\left[-\frac{r h'(1/n^*)}{k_B T}\right] \left[1 + O\left(\frac{1}{r}\right)\right].\quad (59)$$

The $O(1/r)$ term comes from subleading corrections to $G_{2m}(r)$ that we have chosen not to calculate explicitly. The location n^* of the saddle point satisfies $h'(1/n^*) = (n^*)[h(n^*) + g_0/2]$, where $h'(x) \equiv dh/dx$ plays the role of a force. Indeed, upon using the Legendre transform relation between h and g , we find that $h'(1/n^*) = F_c$. Thus, for large r , the average force in the constant extension ensemble takes the simple form

$$\langle F \rangle = -k_B T \frac{\partial \ln \mathcal{Z}}{\partial r} \simeq F_c + O\left(\frac{1}{r^2}\right).\quad (60)$$

In the constant force ensemble, on the other hand, $\langle r \rangle \propto 1/f \sim 1/(F_c - F)$, which upon inversion gives the slower approach to $F_c F = F_c + O(1/r)$. Both ensembles predict that complete unzipping of the dsDNA occurs at $F = F_c$; in fact, in the limit $r \rightarrow \infty$, the constant extension ensemble simply demonstrates coexistence of the bulk unzipped and zipped phases, as in any first-order transition. The approach to $F = F_c$ as r becomes large, however, is markedly different. Equivalence of ensembles exists only in the ‘‘thermodynamic limit’’ $r \rightarrow \infty$.

Because DNA unzipping does not show self-averaging, the situation becomes even more complicated when sequence randomness is introduced. In the constant force ensemble, $\langle m \rangle$ (and hence $\langle r \rangle$) increases monotonically as F increases, for any DNA sequence. In the constant extension ensemble, in contrast, we expect large regions where $d\mathcal{E}/dm$, which plays roughly the role of g_0 , is smaller than average; when the unzipping fork enters one of these regions, $\langle F \rangle$ should decrease. Precisely such behavior is observed in experiments and simulations on the unzipping of lambda phage DNA [21]: $\langle F \rangle$ is seen to vary randomly about an average value as r is increased. For a given random sequence, the functions $\langle r \rangle(F)$ and $\langle F \rangle(r)$ thus cannot be inverses of each other.

One can still ask, however, whether the disorder averages $\overline{\langle r \rangle}(F)$ and $\overline{\langle F \rangle}(r)$ are simply related. Once sequence heterogeneity is present, a term proportional to $W(m)$ [see Eq. (52)] must be incorporated into $\mathcal{Z}(r)$. In analogy to Eqs. (58) and (59), one finds

$$\begin{aligned}\mathcal{Z}(r) &\simeq \int_0^\infty \frac{dm}{m^{1/2}} \exp\left[-\frac{2m}{k_B T} h\left(\frac{r}{2m}\right) - \frac{g_0 m}{k_B T} - \frac{W(m)}{k_B T}\right] \\ &\simeq \sqrt{r} \exp\left[-\frac{x F_c}{k_B T} - \frac{\sqrt{r} W(n^*)}{\sqrt{2} k_B T}\right] \int_{-\infty}^\infty \frac{dn}{(n)^{1/2}} \\ &\quad \times \exp\left[-\frac{r k(n-n^*)^2}{2 k_B T} - \frac{\sqrt{r} W(n-n^*)}{\sqrt{2} k_B T}\right],\end{aligned}\quad (61)$$

where $k = (1/n^*)^3 h''(1/n^*)$. In passing from the first to the second expression, we have used the scaling properties of a random walk to make the substitution, valid on the level of statistical distributions, $W(rn/2) = \sqrt{r/2} W(n)$. We have also expanded around the location n^* of the saddle point in the *nonrandom* case. Because the average terms in the exponential grow as r , while the coefficient of $W(n)$ is only proportional to \sqrt{r} , this expansion will still give the correct asymptotic behavior as $r \rightarrow \infty$.

Equation (62) shows that the leading corrections to $\overline{\langle F \rangle}(r)$ can be described by the equilibrium extension of a spring ‘‘dragged’’ across a random potential [19]. One can estimate the spring’s extension by balancing the elastic energy cost of extension $-rk(n-n^*)^2/2$ with the typical random energy gain $\sqrt{r} W(n-n^*) \sim \sqrt{r} \Delta |n-n^*|$. These two terms are of the same order when $|n-n^*| \sim (\Delta/k^2 r)^{1/3}$. The typical energy gain due to extension is then $\sqrt{r} \Delta (n-n^*) \sim (\Delta^2 r/k)^{1/3}$; note that although $n-n^*$ is positive or negative with equal probability, the associated change in energy must always be negative. We thus expect that the disorder-averaged free energy should behave as

$$-k_B T \overline{\ln \mathcal{Z}(r)} \sim r F_c - \left(\frac{\Delta^2 r}{k}\right)^{1/3}.\quad (62)$$

Note that the term proportional to $W(n^*)$ averages to zero. Upon taking a derivative with respect to r , one concludes that the disorder-averaged force in the constant extension ensemble approaches F_c for large r according to

$$F_c - \overline{\langle F \rangle}(r) \sim \left(\frac{\Delta^2}{k}\right)^{1/3} \frac{1}{r^{2/3}}.\quad (63)$$

In contrast, in the constant force ensemble, $\overline{\langle r \rangle} \sim \overline{\langle m \rangle} \sim 1/(F_c - F)^2$, which upon inversion gives $F_c - F \sim 1/\overline{\langle r \rangle}^{1/2}$. Once again, the two ensembles agree *only* on the location of the unzipping transition.

There is one further, more subtle relationship between the two ensembles with sequence randomness. For a given sequence, the constant force partition function can be written in either of two ways:

$$\begin{aligned}Z(F) &= \int_0^\infty dm \exp\left[-\frac{W(m) + fm}{k_B T}\right] = \int_{-\infty}^\infty dr \\ &\quad \times \exp\left[-\frac{\delta \mathcal{F}(r) + (F_c - F)r}{k_B T}\right],\end{aligned}\quad (64)$$

where $\delta\mathcal{F}(r) \equiv -k_B T \ln[Z(r)] - F_c r$. These two expressions must of course ultimately lead to the same result, and this fact has interesting consequences for the properties of $\delta\mathcal{F}$. Near the unzipping transition, $f = 2g(F) - g_0 \sim 2g'(F_c)(F - F_c) = 2|g'(F_c)|(F_c - F)$. Up to a constant factor (and neglecting exponentially suppressed contributions to the second integral from $r < 0$), both expressions for $Z(F)$ can thus be viewed as Laplace transforms with respect to the same variable. Hence, we expect that $\delta\mathcal{F}(r)$ must have statistics very similar to those of $W(m)$. In particular, for small $F_c - F$, the integral with respect to r , like the one with respect to m , is likely to be dominated by its absolute minimum. In order to give the correct sequence of plateaus and jumps, $\delta\mathcal{F}(r)$ should thus behave like a random walk for large r , with $(\delta\mathcal{F}(r') - \delta\mathcal{F}(r))^2 \approx 2|g'(F_c)|\Delta|r' - r|$. Scaling arguments due to Gerland *et al.* [19] suggest that the force deviation $\delta F(r) \equiv \langle F(r) \rangle - F_c = \partial\delta\mathcal{F}/\partial r$ should have a variance that decays as $\overline{\delta F(r)^2} \sim \Delta^{1/3}(k/r)^{2/3}$. For $(\delta\mathcal{F}(r') - \delta\mathcal{F}(r))^2$ to behave correctly at large scales, $\delta F(r)$ must then have a correlation length that grows as $r^{2/3}$. One plausible explanation for this behavior is that, much as in the constant force ensemble, n locks into a single minimum of $W(n)$ as r is increased over a finite interval before jumping to a new minimum, with the size of this interval increasing as r grows larger.

VII. DYNAMICS

So far, we have only considered static, equilibrium behavior. In real experimental systems, of course, dynamical effects can play an important role. The complete description of the dynamics of the unzipping transition, allowing for the possibility of thermally activated denaturation bubbles in the bulk dsDNA, is a challenging and still open problem. Four time scales come into play: the time scales τ_{end} and τ_{bulk} of base pairing and unpairing at the end of a double-stranded region and in the bulk, the relaxation time $\tau_{\text{ss}}(m)$ of the liberated single strands, and the rotational relaxation time $\tau_{\text{rot}}(m)$ of the still zipped dsDNA, which because of its helical structure develops excess twist as it is unravelled from one end. The latter two time scales are expected to depend on m . Cocco *et al.* [14] have suggested that there may be a fifth scale associated with overcoming an additional energy barrier to unzipping the first few bases of an initially blunt-ended dsDNA, but such a barrier would not affect the long time unzipping dynamics. Although not the subject of extensive investigation, the opening rate τ_{end} of terminal base pairs is thought to be between 1 and 10 msec [14,59]. Because opening a base pair in the middle of a double-stranded region requires overcoming *two* stacking interactions, instead of one for opening at the end, we expect $\tau_{\text{bulk}} \gg \tau_{\text{end}}$ [14,53]; in unzipping experiments, the pulling force will further accelerate base-pair opening at the unzipping fork. Marenduzzo *et al.* [12] have argued that the relaxation time of the ssDNA is given by the time required to move the entire single strand a distance x for each monomer that is opened or closed. Because the forces required to denature dsDNA are fairly large, each single-stranded monomer will be under considerable tension, with the average extension x per mono-

mer of order the monomer size a . The mobility of a single strand of length m is then of order $1/4\pi\eta am$, where η is the solvent viscosity, regardless of whether the strand is described by the Rouse or by the Zimm model. Assuming a force F of order 10 pN, one then finds that $\tau_{\text{ss}}(m) \sim 4\pi\eta a^2 m/F \sim (1 \text{ nsec})m$. Similarly, we can estimate the rotational relaxation time τ_{rot} of a dsDNA molecule of length $(N-m)$ by finding the time for it to turn through $2\pi/10.5$ rad (with the denominator of 10.5 arising from the number of base pairs per helix turn in B form DNA in solution [54]). For a dsDNA strand of radius 1 nm, the torque exerted by the two single strands under tension is roughly $2 \times 10 \text{ pN} \times 1 \text{ nm} = 20 \text{ pN nm}$. Classically, the rotational mobility μ_{rot} of a dsDNA molecule of length N has been calculated by assuming it is a straight, rigid rod, yielding the value $\mu_{\text{rot}} \approx (2 \times 10^{-8} \text{ sec/g cm}^2)N$ [55]; this would imply $\tau_{\text{rot}} \sim (3 \text{ nsec})(N-m)$. More recently, Nelson has argued that the presence of intrinsic bends in natural dsDNA could decrease the rotational mobility, and thus increase τ_{rot} , by several orders of magnitude [56].

The time dependence of the number of unzipped bases $m(t)$ will be determined by which of these four time scales is the slowest. The most difficult situation to analyze occurs if the system is dominated by τ_{bulk} , as can be the case for small enough m and N . In this case, the dynamics of the denaturation bubbles in the bulk dsDNA will be slower than the dynamics of the actual unzipping. Unlike in our equilibrium calculations, the bubbles then cannot be integrated out to give an effective (local) dynamics that depends only on m . Indeed, in the limit that bases at the unzipping fork open much faster than those in the bulk, the unzipping fork will propagate into an almost frozen landscape of opened and closed base pairs. Strongly nonequilibrium effects, including a depression of the effective F_c , could then become visible [57]. The predicted decrease in the apparent critical force has a simple origin: The base pairs' fluctuations between open and closed contribute some entropy to the dsDNA's average free energy g_0 , making g_0 more negative (and thus the dsDNA more stable) than it would otherwise be. On time scales such that these fluctuations are frozen out, this entropy is lost, the dsDNA appears less stable, and F_c decreases. Because $\tau_{\text{ss}}(m)$ grows with m , it must eventually become slower than τ_{bulk} ; beyond this point, more conventional behavior should reemerge.

Fortunately, in physiological conditions, opening of base pairs in bulk dsDNA is extremely rare. Well below the melting temperature, it is then reasonable to assume that all base pairs beyond the unzipping fork are closed, and to focus only on the position of the unzipping fork. Consider first the case in which the slowest of the three remaining time scales is independent of m , either because τ_{end} is the slowest (as will be the case for $m < N \lesssim 10^3$ or 10^4 under the assumption of a straight rod rotational mobility for dsDNA) or because τ_{rot} is the slowest, but with $m \ll N$ so that changes in m have a negligible effect on τ_{rot} . In this regime, the unzipping dynamics is dominated by the diffusion of the unzipping fork in the one-dimensional energy landscape $\mathcal{E}(m)$. In other words, it is an example of the well-studied problem of a random walk in a random force field, sometimes known as the Sinai

problem [25] (for reviews, see [26]). The overdamped dynamics associated with the continuum free energy of Eq. (13) then takes the form

$$\frac{dm}{dt} = -\Gamma \frac{\delta \mathcal{E}(m)}{\delta m} + \zeta(t) = -\Gamma [f + \eta(m)] + \zeta(t), \quad (65)$$

where the effect of thermal fluctuations is included through the noise source $\zeta(t)$ with correlations

$$\langle \zeta(t) \zeta(t') \rangle = 2k_B T \Gamma \delta(t - t'). \quad (66)$$

The magnitude of the phenomenological drag coefficient Γ is set by the slowest time scale:

$$\Gamma = \frac{1}{\tau k_B T}, \quad (67)$$

with τ equal to τ_{end} or τ_{rot} as appropriate. We expect that Eq. (65) describes the dynamics of the unzipping fork at long times for small f . In the absence of sequence heterogeneity [$\eta(m) = 0$], it yields simple diffusion with drift above the unzipping transition,

$$\langle m(t) \rangle = (\Gamma |f|) t \quad \text{and} \quad \langle [m(t) - \langle m(t) \rangle]^2 \rangle = (\Gamma k_B T) t. \quad (68)$$

In contrast, in the presence of sequence heterogeneity, the long time dynamics is determined by large energy barriers that grow with m ; a number of rigorously established results can then be reproduced by simple physical arguments [26,50,57]. For example, when $F = F_c$ (i.e., $f = 0$), $\mathcal{E}(m) \sim \sqrt{\Delta m}$; taking this to be a typical barrier size, one finds that the time to go a distance m is $t \sim \tau \exp(\sqrt{\Delta m}/k_B T)$, suggesting that $m(t)$ is typically of order $\ln^2(t/\tau)$. Indeed, it is known that in the presence of a single reflecting wall (in our case, the end from which the semi-infinite duplex is being unzipped), the ratio $m(t)/\ln^2(t/\tau)$ approaches a t -independent limiting distribution at large times [50]. Similarly, just *below* the unzipping transition, the unzipping fork is essentially always in a region where the small bias f can be ignored. Given that $m_{\text{jump}} \sim \langle m \rangle \sim \Delta/f^2$, we expect that the typical time to equilibrate at a bias f (and in particular to jump from one local minimum to a new minimum with lower energy as f is decreased) should be of order $\tau \exp(\Delta/f k_B T)$, a result that is supported, up to logarithmic factors, by renormalization group calculations [50].

Just *above* F_c , the dsDNA must eventually unzip completely, but the propagation of the unzipping fork is again dramatically slowed by the presence of large energy barriers. The distribution of barrier heights is known to have exponential tails [60], leading to a distribution of trapping times T that decays as $1/T^{\mu+1}$, with

$$\mu = 2k_B T |f| / \Delta. \quad (69)$$

This same exponent appeared, for example, in Eq. (38), and is known more generally to control the probability of large excursions of a biased random walk [e.g., $\mathcal{E}(m)$] against its

bias [61]. The time to open m base pairs is a sum of $O(m)$ such trapping times, with each time chosen independently. For $\mu < 1$, the median value of this sum grows as $m^{1/\mu}$, so one has sublinear growth with time of the sequence-averaged degree of unzipping,

$$\overline{\langle m(t) \rangle} \sim t^\mu \quad (\mu < 1). \quad (70)$$

The average extent of unzipping $\langle m(t) \rangle$ of a given polynucleotide is typically also of order t^μ , but with time and sequence-dependent fluctuations in the prefactor. For $1 < \mu < 2$, $\langle m(t) \rangle \sim t$ recovers its usual behavior, but there is still anomalous behavior in the second cumulant: $\langle m(t)^2 \rangle - \langle m(t) \rangle^2$ typically grows as $t^{2\mu}$. Conventional diffusion with drift is recovered only for forces large enough that $\mu > 2$, or $|f| > \Delta/k_B T \sim O(k_B T)$ for dsDNA in physiological conditions. For the freely jointed chain expression (7) for $g(F)$, this condition translates to $F - F_c \gtrsim 5$ pN; there is thus a substantial window where anomalous drift can be observed in a single molecule experiment. Just as for the equilibrium results discussed earlier in this paper, most of the qualitative features of the unzipping dynamics for uncorrelated random sequences also apply to the unzipping of correlated random sequences, albeit with different exponents [62].

These results have interesting implications for attempts to read sequence information via experiments that monitor the velocity dm/dt of the unzipping fork for a fixed force $F > F_c$. Read naively, Eq. (65) suggests that the coarse-grained sequence fluctuations embodied in $\eta(m)$ and the thermal noise $\zeta(t)$ will together modulate a mean unzipping velocity $\langle dm/dt \rangle = \Gamma |f|$. This picture is certainly correct sufficiently far above the unzipping transition, where deep traps in the energy landscape are rare. However, we can estimate that thermal fluctuations will obscure the sequence-dependent modulation of the mean velocity whenever

$$\langle \zeta(t) \zeta(t') \rangle \gg \Gamma^2 \overline{\eta(\Gamma |f| t) \eta(\Gamma |f| t')}, \quad (71)$$

where we have used the zeroth-order relation

$$m(t) \approx \Gamma f t \quad (72)$$

to approximate $m(t)$. Equations (14) and (66) then show that thermal noise can only be neglected provided

$$2k_B T \Gamma \ll \frac{\Gamma \Delta}{|f|}, \quad (73)$$

or for

$$\mu = \frac{2k_B T |f|}{\Delta} \ll 1. \quad (74)$$

In this regime, however, the approximation (72) breaks down; indeed, we have seen that for $\mu < 1$, the dynamics is dominated by the presence of deep traps in the energy landscape, with $m(t) \sim t^\mu$. Efforts to extract sequence informa-

tion from dm/dt in this regime will be seriously hampered by the slow, erratic dynamics associated with energy barriers of order $\sqrt{\Delta m}$.

The results discussed above are valid as long as the slowest time scale τ is roughly independent of m . If m dependence becomes important, large energy barriers still dominate the dynamics, but our arguments must be modified to account for this new feature [12]. Thus, for example, if m becomes large enough, the relaxation of the single strands will set the basic scale for the dynamics. Exactly at the transition, we then expect $t \sim m \exp(\sqrt{\Delta m}/k_B T)$ (the prefactor of m arising from the fact that $\tau_{ss} \sim m$); this yields exactly the same very slow asymptotic behavior $\langle m \rangle \sim \ln^2(t)$ as before. Likewise, the equilibration times below the transition remain unchanged. On the other hand, for $F > F_c$, new behavior emerges. The time to go a distance m is now of order $\sum_{n=0}^m n T_n$, with each of the T_n chosen from the same distribution with tails like $1/T_n^{\mu+1}$. The median of the distribution of this new sum occurs at a time of order $m^{(\mu+1)/\mu}$, suggesting $\langle m \rangle(t) \sim t^{\mu/(\mu+1)}$. As hypothesized in Ref. [12], the scaling laws in this regime are thus related to those for $\tau_{ss}(m) < \tau_{end}$ by the substitution $t \rightarrow t/x$. Similarly, when $\tau_{rot}(m) \sim N - m$ is the slowest time scale, the logarithmic growth at or below the transition remains unchanged, while above the transition an analysis of a sum of trapping times $\sum_{n=0}^m (N - n) T_n$ suggests $\langle m \rangle(t) \sim N [1 - (1 - kt^\mu/N^{\mu+1})^{1/(\mu+1)}]$, with k an undetermined constant. Thus, the fact that τ_{ss} and τ_{rot} depend on m does not change the essential physical result that sequence randomness leads to large energy barriers, and thus to a substantial slowing down of unzipping.

VIII. CONCLUSIONS

In this paper, we have given a detailed theoretical analysis of a simple micromechanical experiment: the mechanical denaturation, or unzipping, of double-stranded DNA with a random base sequence. Although of current experimental interest in its own right, this system can also serve as a springboard for developing ideas with potential applications to micromanipulation experiments on more structurally complicated biomolecules. Several such ideas emerged from our study. On the most basic level, the constant force and constant extension ensembles were shown to give different force-extension curves in single molecule experiments. We argued that unzipping in the constant force ensemble can always be described by a one-dimensional free-energy landscape $\mathcal{E}(m)$, with an average slope $f = 2g(F) - g_0$ set by the applied force F and F -independent fluctuations about this average determined by the structure and sequence of the molecule being examined. The number of monomers $\langle m \rangle$ liberated at a given F is then simply an equilibrium average over m with weight $\exp[-\mathcal{E}(m)/k_B T]$. Once sequence variation is present, $\mathcal{E}(m)$ will in general pass below zero for small enough $f > 0$. Partial mechanical denaturation then allows the liberated monomers to gain more free energy by aligning with the applied force than they lose by breaking native contacts. For small f , $\langle m \rangle$ should be dominated by the deepest minima in $\mathcal{E}(m)$.

For the particular case of unzipping a single dsDNA molecule, these qualitative observations can be given more precise meaning. The energy function $\mathcal{E}(m)$ then behaves like a biased random walk on scales beyond a few bases. When the pulling force F is increased to a critical value F_c , the bias changes sign, and a phase transition occurs. Randomness is always relevant at this wettinglike transition, with the average number of broken base pairs $\langle m \rangle$ diverging as $1/(F_c - F)$ for homopolymer duplexes, but as $1/(F_c - F)^2$ in the presence of a random sequence. Individual dsDNA molecules approaching the unzipping transition open in a sequence of sharp jumps, separated by long plateaus in which $\langle m \rangle$ remains essentially constant. The jumps become sharper and sharper as $f \rightarrow 0$. For small f , $\langle m \rangle$ for any given polymer must approach the absolute minimum of $\mathcal{E}(m)$. The plateaus and jumps can then be understood as arising from a sequence of minima. A given minimum remains stable over a range of f values. As the bias f decreases, however, eventually a new minimum at larger m will become lower in energy; at this point, $\langle m \rangle$ will jump to the new minimum. Starting from this picture, we were able to make precise predictions about statistical features of single molecule unzipping such as the distribution of jump sizes m_{jump} . These showed good agreement with simulations. The distribution of m_{jump} also revealed that the correlation between $\langle m \rangle$ at different values f_1 and $f_2 < f_1$ of f vanishes for small f_2/f_1 . As a result, even though $\langle m \rangle$ can differ significantly from $\overline{\langle m \rangle}$ at any single force value, a plot of $\langle m \rangle$ versus f for a given random sequence still shows the same scaling behavior as does the average over many sequences $\overline{\langle m \rangle}$. Several of these features, most notably the dominance of the absolute minimum, are known to occur more generally in random systems; indeed, an added interest of DNA unzipping is that it is a physical realization of one of the simplest models in the statistical mechanics and dynamics of random systems [25,26,44]. Similar conclusions should apply to experiments on the unzipping of individual RNA hairpins [3], although experiments on longer hairpins would be required to provide a complete test of the theory.

Although the predictions for DNA unzipping do not apply directly to micromechanical assays on systems such as proteins [4] or the complex RNA folds of naturally occurring ribozymes [3], they do suggest a definite agenda for understanding such experiments. In varying the pulling force F in the constant force ensemble, one is essentially searching for local minima along the denaturation pathway; each observed plateau corresponds to a state that is metastable at zero force, but is stabilized in an appropriate range of F values. If $g(F)$ can be determined from measurements on unfolded strands, then the energies of the original metastable states are easily inferred from the forces at which jumps occur. Related ideas have been applied with great success to the interpretation of micromanipulation experiments on individual ‘‘lock and key’’ bonds [63].

This picture of plateaus and jumps could break down if, instead of traversing only a single pathway, the mechanical denaturation can proceed along one of many different routes [19]. For example, in micromanipulation experiments on folded RNA's, it can transpire that a series of many hair-

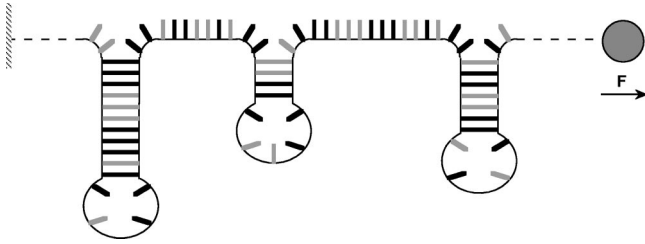


FIG. 18. Sketch of several RNA stems being opened in parallel, as might occur in a micromechanical experiment on a ribozyme or other folded RNA molecule. If each stem has an independently chosen random sequence, then in the limit of a large number of long stems, the number of unzipped bases will equal the disorder-averaged value $\overline{\langle m \rangle}$. The measured force-extension curve must then be smooth and monotonic in any ensemble.

pins are under tension simultaneously, as in Fig. 18. In the constant force ensemble, if there are M long hairpins with independently chosen random sequences, the average extension $\langle r \rangle$ will be simply the sum of M independent single hairpin extensions. As a function of f , each of these single hairpins will go through its own sequence of plateaus and jumps. Each time a particular hairpin has a jump, $\langle r \rangle$ will also jump, but the typical jump size will be $\langle r \rangle / M$ instead of $\langle r \rangle$. Similarly, the plateaus in $\langle r \rangle$ will be shortened: The probability that none of the single hairpins jump as f is decreased from f_1 to f_2 is $(f_2/f_1)^M$, which decays very quickly for large M . As M increases, shorter and shorter jumps and plateaus will eventually merge into a smooth curve. Indeed, one expects that as $M \rightarrow \infty$, $\langle r \rangle \rightarrow M \langle r \rangle + O(\sqrt{M})$. That is, a system of many hairpins should exhibit self-averaging. Moreover, because the limit of many hairpins is essentially a thermodynamic limit, equivalence of ensembles must also be recovered. In fact, the force-extension curve in the constant extension ensemble must approach the disorder-averaged curve for the constant force ensemble as M becomes large. In physical terms, there must be a constant tension along the entire chain of hairpins; in the limit of many hairpins, each one sees this tension rather than the extension imposed on the entire chain. Once there are enough competing hairpins, any equilibrium experiment will give the same smooth curve. Such smoothing, with its attendant loss of structural information, has recently been observed in simulations [19]. Both the continuous increase of the disorder average and the plateaus and jumps of a single hairpin can thus appear in single molecule experiments.

We note in conclusion that the ideas from the physics of one-dimensional disordered systems applied here to mechanical denaturation experiments may find applications elsewhere in biophysics. To cite one example, the DNA-binding protein recA adheres with a binding affinity that depends strongly on the nucleotide sequence [64]. When ATP is replaced by the nonhydrolyzable analog ATP- γ S, allowing the system to reach equilibrium, the position of the pointlike polymerization boundary separating domains of polymerized recA from bare DNA can be described by a coarse-grained model like Eqs. (13)–(15). Similarly, the motion of a single boundary during polymerization can be described as biased

diffusion in a random force field, and one might expect in appropriate parameter ranges to find strong disorder-induced slowing of the sort discussed in Sec. VII. More generally, the kinetics of multiple polymerization boundaries (associated with multiple recA domains) on a single long polynucleotide can naturally be mapped to the dynamics of kinks in a one-dimensional random field Ising model, which is known to be in the Sinai universality class [25,26]. Although the relevance of such anomalous dynamics to the functioning of biological systems *in vivo* remains to be established, these effects may play a role in a number of *in vitro* assays.

ACKNOWLEDGMENTS

It is a pleasure to thank Jean-Philippe Bouchaud, Ralf Bundschuh, Daniel Branton, Daniel Fisher, Ulrich Gerland, Terry Hwa, and Hervé Isambert for helpful conversations and Roy Bar-Ziv and Albert Libchaber for introducing us to recA polymerization. This research was supported by the NSF through grant DMR97-14725 and through the Harvard MRSEC via grant DMR98-09363. Work at the University of California, Santa Barbara was supported by NSF Grant No. PHY99-07949.

APPENDIX: SIMULATION METHODOLOGY

This appendix describes the numerical method used to generate the data points in Figs. 8–13. The simulations were performed on a simplified model of dsDNA in which all $A-T$ base pairs have a pairing energy ε_{AT} and all $G-C$ base pairs a pairing energy ε_{GC} [21]. In contrast to the convention of Sec. II A, here we define pairing energies as the free energy difference between the bound base pair and the two monomers subject to the tension F . The average pairing energy of the sequence is thus f . All base pairs other than the m unzipped bases are assumed to be closed, an excellent approximation for dsDNA in physiological conditions. We are interested primarily in behavior near the unzipping transition, where many bases have been unzipped. In this regime, most of our predictions depend only on universal properties of random walks, so the simplifications in our model are justified. Our results are always reported in terms of the parameters f and Δ that can be defined with reference only to the large m behavior of $\mathcal{E}(m)$. We assume for simplicity that $A-T$ and $G-C$ pairs occur with equal probability 1/2, and we take the pairing energies to be $\varepsilon_{AT} = f - \sqrt{\Delta}$ and $\varepsilon_{GC} = f + \sqrt{\Delta}$. The disorder strength Δ is usually chosen to be between 1 and 9, while f varies from 1 down to a lower bound determined by demanding that $\overline{\langle m \rangle} \approx \Delta / (2f^2) \leq N/8$. Here N is the total number of base pairs in the dsDNA, which we usually choose to fall between 5×10^5 and 5×10^6 . For a given sequence $\{\varepsilon_i\}$, with each ε_i equal to either ε_{AT} or ε_{GC} , $\mathcal{E}(m)$ takes the form $\mathcal{E}(m) = \sum_{i=1}^m \varepsilon_i$. The average and variance of \mathcal{E} are then $\overline{\mathcal{E}(m)} = mf$ and $\overline{\mathcal{E}(m)^2} - \overline{\mathcal{E}(m)}^2 = \Delta m$, allowing direct contact with the continuum limit described by Eqs. (13) and (14). The temperature $k_B T$ is set to one.

Our one-dimensional system is sufficiently simple that it is possible to proceed by direct evaluation of the partition function $Z = \sum_{m=0}^N \exp[-\mathcal{E}(m)]$ and the average number of

unzipped bases $\langle m \rangle = \sum_{m=0}^N m \exp[-\mathcal{E}(m)]/Z$. For each random sequence, successive values of ε_i are chosen at random, starting with ε_N . The running sums $Z_i \equiv \sum_{m=i}^N \exp[-\mathcal{E}(m) + \mathcal{E}(i-1)]$ and $\langle m \rangle_i \equiv \sum_{m=i}^N m \exp[-\mathcal{E}(m) + \mathcal{E}(i-1)]$ are then updated according to $Z_i = \exp(-\varepsilon_i)(1+Z_{i+1})$ and $\langle m \rangle_i = \exp(-\varepsilon_i)(i + \langle m \rangle_{i+1})$; once the sum is complete, $\langle m \rangle$ is normalized by dividing by Z . We keep separate sums for each value of f , and, at each i , update each of them with the same random choice of ε_{AT} or ε_{GC} . In some runs, we also kept track of the running sum of ε_i and of the location of the deepest minimum encountered up to position i .

The binned data in Figs. 11 and 12 represent the output of several thousand runs with independently chosen random sequences and varying values of Δ and N . In Fig. 11, which plots the distribution of $\langle m \rangle$, data points for each value of f from each run were rescaled appropriately and used together to construct the histogram. Similarly, all pairs of points with $f_2/f_1 \approx 0.77$ were rescaled and used in making the histogram of m_{jump} in Fig. 12; in order to account for the predicted δ function at $m_{\text{jump}}=0$, a fraction f_2/f_1 of the total number of data points was subtracted from the number of counts in the bin that included $m_{\text{jump}}=0$.

-
- [1] P. Cluzel, M. Surette, and S. Leibler, *Science* **287**, 1652 (2000).
- [2] T. T. Perkins, D. E. Smith, and S. Chu, *Science* **276**, 2016 (1997).
- [3] J. Liphardt, B. Onoa, S. B. Smith, I. Tinoco, and C. Bustamante, *Science* **292**, 733 (2001).
- [4] M. Rief, M. Gautel, F. Oesterhelt, J. M. Fernandez, and H. E. Gaub, *Science* **276**, 1109 (1997); M. S. Z. Kellermayer, S. B. Smith, H. L. Granzier, and C. Bustamante, *ibid.* **276**, 1112 (1997); L. Tskhovrebova, J. Trinick, J. A. Sleep, and R. M. Simmons, *Nature (London)* **387**, 308 (1997).
- [5] D. K. Lubensky and D. R. Nelson, *Phys. Rev. Lett.* **85**, 1572 (2000).
- [6] C.-K. Peng, S. V. Buldyrev, A. L. Goldberger, F. Sciortino, M. Simons, and H. E. Stanley, *Nature (London)* **356**, 168 (1992); A. Arneodo, E. Bacry, P. V. Graves, and J.-F. Muzy, *Phys. Rev. Lett.* **74**, 3293 (1995); S. V. Buldyrev *et al.*, *Phys. Rev. E* **51**, 5084 (1995).
- [7] R. E. Thompson and E. D. Siggia, *Europhys. Lett.* **31**, 335 (1995).
- [8] M. Peyrard, *Europhys. Lett.* **44**, 271 (1998).
- [9] S. M. Bhattacharjee, *J. Phys. A* **48**, L423 (2000).
- [10] K. L. Sebastian, *Phys. Rev. E* **62**, 1128 (2000).
- [11] D. Marenduzzo, A. Trovato, and A. Maritan, *Phys. Rev. E* **64**, 031901 (2001).
- [12] D. Marenduzzo, S. M. Bhattacharjee, A. Maritan, E. Orlandini, and F. Seno, *Phys. Rev. Lett.* **88**, 028102 (2002).
- [13] S. M. Bhattacharjee and D. Marenduzzo, e-print cond-mat/0106110.
- [14] S. Cocco, R. Monasson, and J. F. Marko, *Proc. Natl. Acad. Sci. U.S.A.* **98**, 8608 (2001).
- [15] E. Mukamel and E. I. Shakhnovich, e-print cond-mat/0108447.
- [16] A. Montanari and M. Mezard, *Phys. Rev. Lett.* **86**, 2178 (2001).
- [17] H. Zhou, Y. Zhang, and Z.-C. Ou-Yang, *Phys. Rev. Lett.* **86**, 356 (2001).
- [18] H. Zhou and Y. Zhang, *J. Chem. Phys.* **114**, 8694 (2001).
- [19] U. Gerland, R. Bundschuh, and T. Hwa, *Biophys. J.* **81**, 1324 (2001).
- [20] G. U. Lee, L. A. Chrisey, and R. J. Colton, *Science* **266**, 771 (1994).
- [21] B. Essevaz-Roulet, U. Bockelmann, and F. Heslot, *Proc. Natl. Acad. Sci. U.S.A.* **94**, 11 935 (1997); U. Bockelmann, B. Essevaz-Roulet, and F. Heslot, *Phys. Rev. Lett.* **79**, 4489 (1997); *Phys. Rev. E* **58**, 2386 (1998).
- [22] M. Rief, H. Clausen-Schaumann, and H. E. Gaub, *Nat. Struct. Biol.* **6**, 346 (1999); H. Clausen-Schaumann, M. Rief, C. Tolksdorf, and H. E. Gaub, *Biophys. J.* **78**, 1997 (2000).
- [23] T. Strunz, K. Oroszlan, R. Schäfer, and H.-J. Güntherodt, *Proc. Natl. Acad. Sci. U.S.A.* **96**, 11 277 (1999); L. H. Pope, M. C. Davies, C. A. Laughton, C. J. Roberts, S. J. B. Tendler, and P. M. Williams, *Eur. Biophys. J.* **30**, 53 (2001).
- [24] D. Wirtz, *Phys. Rev. Lett.* **75**, 2436 (1995); F. Amblard, B. Yurke, A. Pargellis, and S. Leibler, *Rev. Sci. Instrum.* **67**, 818 (1996).
- [25] Ya. G. Sinai, *Theor. Probab. Appl.* **27**, 247 (1982).
- [26] J.-P. Bouchaud and A. Georges, *Phys. Rep.* **195**, 127 (1990); J.-P. Bouchaud, A. Comtet, A. Georges, and P. le Doussal, *Ann. Phys. (N.Y.)* **201**, 285 (1990).
- [27] K. Visscher and S. M. Block, *Methods Enzymol.* **298**, 460 (1998); A. F. Oberhauser, P. K. Hansma, M. Carrion-Vasquez, and J. M. Fernandez, *Proc. Natl. Acad. Sci. U.S.A.* **98**, 468 (2001).
- [28] S. Dietrich, in *Phase Transitions and Critical Phenomena*, edited by C. Domb and J. L. Lebowitz (Academic, London, 1988), Vol. 12, p. 2; G. Forgacs, R. Lipowsky, and T. M. Nieuwenhuizen, in *Phase Transitions and Critical Phenomena*, edited by C. Domb and J. L. Lebowitz (Academic, London, 1991), Vol. 14, p. 135; E. M. Blokhuis and B. Widom, *Curr. Opin. Colloid Interface Sci.* **1**, 424 (1996).
- [29] J. H. Gibbs and E. A. DiMarzio, *J. Chem. Phys.* **30**, 271 (1959); B. H. Zimm, *ibid.* **33**, 1349 (1960); M. E. Fisher, *J. Stat. Phys.* **34**, 667 (1984). For a discussion of effects due to sequence randomness near the zero force thermal denaturation transition, see L.-H. Tang and H. Chaté, *Phys. Rev. Lett.* **86**, 830 (2000) and A. Y. Grosberg and A. R. Khokhlov, *Statistical Physics of Macromolecules* (AIP Press, Woodbury, NY, 1994), Sec. 41, and references therein.
- [30] D. Poland and H. A. Scheraga, *Theory of Helix-Coil Transitions in Biopolymers* (Academic, New York, 1970).
- [31] M. Peyrard and A. R. Bishop, *Phys. Rev. Lett.* **62**, 2755 (1989); D. Cule and T. Hwa, *ibid.* **79**, 2375 (1997).
- [32] M. Doi and S. F. Edwards, *The Theory of Polymer Dynamics* (University Press, Oxford, 1986).
- [33] S. B. Smith, Y. Cui, and C. Bustamante, *Science* **271**, 795 (1996).
- [34] J. SantaLucia, H. T. Allawi, and P. A. Seneviratne, *Biochemistry* **35**, 3555 (1996).

- [35] B. Maier, D. Bensimon, and V. Croquette, Proc. Natl. Acad. Sci. U.S.A. **97**, 12 002 (2000).
- [36] P. Pincus, *Macromolecules* **9**, 386 (1976); see also P. G. de Gennes, *Scaling Concepts in Polymer Physics* (Cornell University Press, Ithaca, 1979).
- [37] D. Branton (personal communication).
- [38] D. K. Lubensky and D. R. Nelson, Biophys. J. **77**, 1824 (1999).
- [39] X. Châtellier, T. J. Senden, J.-F. Joanny, and J.-M. di Meglio, Europhys. Lett. **41**, 303 (1998).
- [40] D. Ertas, Phys. Rev. B **59**, 188 (1999).
- [41] A. O. Parry, C. Rascon, and A. J. Wood, Phys. Rev. Lett. **83**, 5535 (1999).
- [42] N. Hatano and D. R. Nelson, Phys. Rev. Lett. **77**, 570 (1996); Phys. Rev. B **56**, 8651 (1997).
- [43] A. B. Harris, J. Phys. C **7**, 1671 (1974).
- [44] M. Opper, J. Phys. A **26**, L719 (1993); K. Broderix and R. Kree, Europhys. Lett. **32**, 343 (1995); L.-H. Tang, K. Sneppen, and T. Hwa (unpublished).
- [45] C. Monthus and A. Comtet, J. Phys. I **4**, 635 (1994); G. Radons, J. Phys. A **31**, 4141 (1998).
- [46] N. G. van Kampen, *Stochastic Processes in Physics and Chemistry* (Elsevier, Amsterdam, 1992).
- [47] Simulations consisted of exact evaluation of the partition function for randomly generated sequences; details are given in Appendix A.
- [48] A. Comtet, C. Monthus, and M. Yor, J. Appl. Probab. **35**, 255 (1998), and references therein.
- [49] D. S. Fisher and D. A. Huse, Phys. Rev. B **38**, 373 (1988); **38**, 386 (1988); T. Hwa and D. S. Fisher, *ibid.* **49**, 3136 (1994); T. Hwa and D. S. Fisher, Phys. Rev. Lett. **72**, 2466 (1994).
- [50] P. le Doussal, C. Monthus, and D. S. Fisher, Phys. Rev. E **59**, 4795 (1999).
- [51] W. Feller, *An Introduction to Probability Theory and its Applications*, 3rd ed. (Wiley, New York, 1968).
- [52] GenBank NC_001416
- [53] M. D. Frank-Kamenetskii, Phys. Rep. **288**, 13 (1997).
- [54] D. Rhodes and A. Klug, Nature (London) **286**, 573 (1980).
- [55] C. Levinthal and H. R. Crane, Proc. Natl. Acad. Sci. U.S.A. **42**, 436 (1956).
- [56] P. Nelson, Proc. Natl. Acad. Sci. U.S.A. **96**, 14 342 (1999).
- [57] D. S. Fisher (personal communication). For a different perspective on this regime, see Ref. [15].
- [58] I. Tinoco Jr., O. C. Uhlenbeck, and M. D. Levine, Nature (London) **230**, 362 (1971); K. J. Breslauer, R. Frank, H. Blöcker, and L. A. Marky, Proc. Natl. Acad. Sci. U.S.A. **83**, 3746 (1986).
- [59] G. Bonnet, O. Krichevsky, and A. Libchaber, Proc. Natl. Acad. Sci. U.S.A. **95**, 8602 (1998).
- [60] B. Derrida and Y. Pomeau, Phys. Rev. Lett. **48**, 627 (1982).
- [61] S. Karlin and S. F. Altschul, Proc. Natl. Acad. Sci. U.S.A. **87**, 2264 (1990).
- [62] M. V. Feigel'man and V. M. Vinokur, J. Phys. (France) **49**, 1731 (1988).
- [63] R. Merkel, P. Nassoy, A. Leung, K. Ritchie, and E. Evans, Nature (London) **397**, 50 (1999).
- [64] R. Bar-Ziv and A. Libchaber, Proc. Natl. Acad. Sci. U.S.A. **98**, 9068 (2001).